J. Math. Biol. (2017) 74:1425–1482
DOI 10.1007/s00285-016-1060-y

Mathematical Biology

An impulsive modelling framework of fire occurrence in a size-structured model of tree–grass interactions for savanna ecosystems

V. Yatat[1,2,3] · P. Couteron[4,5] · J. J. Tewa[1,2,3] · S. Bowong[2,3,6] · Y. Dumont[7]

Received: 2 May 2015 / Revised: 21 June 2016 / Published online: 22 September 2016

Abstract Fires and mean annual rainfall are major factors that regulate woody and grassy biomasses in savanna ecosystems. Within the savanna biome, conditions of long-lasting coexistence of trees and grasses have been often studied using continuous-time modelling of tree–grass competition. In these studies, fire is a time-continuous forcing while the relationship between woody plant size and fire-sensitivity is not systematically considered. In this paper, we propose a new mathematical framework to model tree–grass interactions that takes into account both the impulsive nature of fire occurrence and size-dependent fire sensitivity (via two classes of woody plants). We carry out a qualitative analysis that highlights ecological thresholds and bifurcation parameters that shape the dynamics of the savanna-like systems within the main ecological zones. Through a qualitative analysis, we show that the impulsive modelling of fire occurrences leads to more diverse behaviors including cases of grassland, savanna and forest tristability and a more realistic array of solutions than the analogous time-continuous fire models. Numerical simulations are carried out with respect to the three

✉ Y. Dumont
yves.dumont@cirad.fr

1 University of Yaoundé I, LIRIMA, GRIMCAPE team, Yaoundé, Cameroon

2 African Center of Excellence in Information and Communication Technologies, University of Yaoundé I, Yaoundé, Cameroon

3 IRD, UMI 209, UMMISCO, IRD France Nord, 93143 Bondy, France

4 IRD, UMR AMAP, Montpellier, France

5 Plant Systematic and Ecology Laboratory, Higher Teachers' Training College, University of Yaoundé I, Yaoundé, Cameroon

6 University of Douala, LIRIMA, GRIMCAPE team, Douala, Cameroon

7 CIRAD, UMR AMAP, Montpellier, France

main ecological contexts (moist, mesic, semi-arid) to illustrate the theoretical results and to support a discussion about the bifurcation parameters and the advantages of the model.

Keywords Savanna · Fire · Asymmetric competition · Impulsive differential equation · Qualitative analysis · Nonstandard finite difference scheme

Mathematics Subject Classification 34K45 · 34K28 · 92D40

1 Introduction

Savannas are ecosystems with fairly continuous grass cover and variable woody cover (Maurin et al. 2014). Savanna-like ecosystems are diverse and cover extensive areas throughout the tropics. Explanations found in the literature about the possible long-lasting coexistence of woody and grassy vegetation components therefore relate to diverse factors and processes depending on the location and the ecological context (Scholes and Archer 1997; Higgins et al. 2000; Bond et al. 2003; Sankaran et al. 2005, 2008; Scheiter and Higgins 2007; Baudena et al. 2014). Several studies have pointed towards the role of stable ecological factors e.g. climate, in shaping the tree to grass ratio along large-scale gradients of rainfall or soil fertility (Sankaran et al. 2005, 2008). Other studies have rather emphasized the reaction of vegetation to recurrent disturbances such as herbivory or fire (Higgins et al. 2000; Van Langevelde et al. 2003; D'Odorico et al. 2006; Sankaran et al. 2008; Smit et al. 2010; Favier et al. 2012 and references therein). Those two points of view are not mutually-exclusive since both environmental control and disturbances may co-occur in a given area and along ecological gradients, although their relative importance generally varies among ecosystems. Bond et al. (2003) proposed the name climate-dependent for ecosystems for which physiognomies are highly dependent on climatic conditions (rainfall, soil moisture) versus disturbance-dependent for ecosystems which dynamics are strongly dependent on fires or herbivores.

Several models using a system of ordinary differential equations (ODE) have been proposed to depict and understand the dynamics of woody and herbaceous components in savanna-like vegetation. A first study (Walker et al. 1981) was orientated towards semi-arid fireless savannas and analyzed the effect of herbivory and drought on the balance between woody and herbaceous biomasses. This model refers to ecosystems immune to fire due to insufficient annual rainfall and grass production. Indeed, fires in savanna-like ecosystems mostly rely on herbaceous biomass that has dried up during the dry season (Higgins et al. 2000; Abbadie et al. 2006, p. 56, Staver et al. 2011; Staver and Levin 2012). As long as yearly rainfall is sufficient, fires impact seedlings and saplings within the flame zone and thus let grasses indirectly inhibit tree establishment (Higgins et al. 2000; Staver et al. 2011; Staver and Levin 2012).

More recently and on the basis of the initial framework of Tilman (1994), that used coupled ODES to model the asymmetric interactions between two kinds of plants, several efforts have been made (see Van Langevelde et al. 2003; Accatino et al. 2010; De Michele et al. 2011; Tchuinté et al. 2014) to model the dynamics of fire-prone

savannas. Indeed, in these works, authors assumed that tree has a direct depressive effect on grass while grass has an indirect (through fires) effect on tree. Moreover, the aforementioned models (Van Langevelde et al. 2003; Accatino et al. 2010; De Michele et al. 2011; Tchuinté et al. 2014) also acknowledged fires as continuous forcing through time.

Based on ecological processes that shape tree–grass interactions in savanna ecosystems (see Scholes and Archer 1997; Scholes 2003), we have developed a time-continuous tree–grass interactions model, called COFAC (COntinuous Fire model of Asymmetric tree–grass Competition) (Yatat et al. 2014). Like Baudena et al. (2010), Staver et al. (2011), we considered in addition to grass, two classes of woody plants: fire-sensitive that are defined as having most of their buds within the flame zone, like seedlings, saplings, shrubs, and fire insensitive which have at least their upperparts above the flame zone, i.e. above ca. 2 m; e.g. Trollope (1996), Van Langevelde et al. (2003), Bond and Keeley (2005). However, in contrast to Staver et al. (2011) and most of the models which have been proposed on the subject (Tilman 1994; Accatino et al. 2010; De Michele et al. 2011; Baudena et al. 2010; Synodinos et al. 2015), we chose to use biomasses as state variables instead of land cover as to account for the fact that plant categories are not mutually exclusive at a given point in space. For instance, grass may exist under tree crowns (Belsky et al. 1989; Belsky 1994; Weltzin and Coughenour 1990; Abbadie et al. 2006; Moustakas et al. 2013). Moreover, results about biomasses directly refer to the cycle of carbon and may directly be assessed from radar remote-sensing in savanna ecosystems (Mermoz et al. 2015). The COFAC lends itself to a complete analytical investigation of its potential outcomes. And contrary to Staver et al. (2011), the COFAC is able to predict as equilibria the full set of vegetation physiognomies that are observed along the whole climatic gradient that is desert and wet tropical forest in addition to grassland and savanna. This was desirable because possible bistability between savanna/grassland and forest is among the empirical facts that are to be accounted for (Hirota et al. 2011; Favier et al. 2012).

However, it is questionable to model fire as a permanent forcing that continuously removes fractions of fire sensitive/prone biomass all over the year, even though several modelling frameworks made this simplification (Van Langevelde et al. 2003; Accatino et al. 2010; De Michele et al. 2011). Indeed, several months and even years can pass between two successive fires, such that fire may be considered as an instantaneous perturbation of the savanna ecosystem. Several recent papers have proposed to model fires as stochastic events while keeping the continuous-time differential equation framework (Baudena et al. 2010; Beckage et al. 2011) or using a time-discrete model (Higgins et al. 2000), Accatino and De Michele (2013), Accatino et al. (2016)).

But in all those models, fire characteristics (intensity and impact on woody plants) remain a linear function of grass biomass which is not satisfactory. Indeed, it is well known that at low grass biomass there is no fires while above a sufficient grass biomass, fires intensity and potential impact on woody individuals increases rapidly before reaching a saturation (Scheiter and Higgins 2007; Staver et al. 2011). Another drawback of the aforementioned recent time-discrete stochastic models (Higgins et al. 2000; Baudena et al. 2010; Beckage et al. 2011) is that they barely lend themselves to analytical (qualitative) approaches.

Therefore, and since we wanted to keep the potential of analytical investigation as large as possible while modelling discrete fires, we turn to the impulsive differential equation modelling framework (Bainov and Simeonov 1995), and propose a new model that features pulse-like periodic phenomena for fires interacting with the overall dynamics of plant growth, decay and competition which remains expressed as in the COFAC by the well-mastered ODE framework. The proposed new model, called IFAC (for Impulsive Fire model of Asymmetric tree–grass Competition) aims therefore to remain analytically tractable as far as possible, while relying on a non-linear system of three coupled impulsive differential equations (IDE) (Bainov and Simeonov 1995), i.e. one equation per vegetation compartment (analogous to COFAC equations) that describes savanna dynamics. Recall that an impulsive differential equation consists on a time-continuous equation and a time-discrete equation. Although impulsive differential equations appear highly relevant to model vegetation dynamics under the influence of punctual disturbances, their use is relatively novel in plant ecology.

Our IFAC aims to acknowledge three major phenomena: the time-discrete occurrence of fire events, the fire-mediated, non-linear negative feedback of grass biomass onto sensitive tree biomass (as in COFAC, see also Staver et al. (2011)) and the asymmetric feed-back of fire insensitive tree biomass on grass biomass, which is a cornerstone of most published savanna models. In addition we also account for direct grass competition on fire sensitive tree biomass (e.g. Scholes and Archer 1997). The structure of the IFAC is formulated and discussed in Sect. 2. In Sect. 3 we reach qualitative analytical results for IFAC through which we highlight some meaningful ecological thresholds that summarize savanna dynamics under impulsive fires. We present a nonstandard numerical scheme for the IFAC in Sect. 4 that ensures full consistency between simulations and analytical results. Moreover, in Sect. 4 we refer to the three main ecological contexts observed in Africa along the rainfall gradient, namely semi-arid, mesic and humid situations as to delineate from existing literature sources-ranges of parameters that depict each context with sufficient accuracy. In Sect. 5, we use these parameter ranges to provide some numerical simulations in order to illustrate the main outcomes and some analytical results.

2 The impulsive fire model of asymmetric tree–grass competition formulation

As briefly mentioned earlier, we make the choice of state variables that express biomasses (in tons/ha) of three interacting vegetation components which are fire sensitive tree (T_S), fire non-sensitive trees (T_{NS}) and grass (G) instead of relative fractions of cover summing to one. This choice departs from several of the published time-continuous models (i.e. Tilman 1994; Accatino et al. 2010; Baudena et al. 2010; De Michele et al. 2011; Synodinos et al. 2015), while it is consistent with the choices of Walker et al. (1981) and Van Langevelde et al. (2003). Expressing biomasses as state variables allows a more straightforward link with field measurements (especially for grasses) and with emerging sources of remotely-sensed data as woody biomass estimates from radar backscattering (Mermoz et al. 2015). Moreover, vegetation components are not mutually exclusive in a given point of space since grass and shrubby

biomasses often exist under a tree crown (Scholes and Archer 1997; Abbadie et al. 2006, p. 156, Moustakas et al. 2013). We also use logistic-like saturation for grass and woody biomasses in contrast to the choice made by Walker et al. (1981) and Van Langevelde et al. (2003). Logistic saturation is widely used in modelling of population dynamics and is of good mathematical tractability while there is limited empirical evidence, if any, to favor a different modelling choice.

Furthermore, we also consider that grass biomass has a direct, depressive effect on the fire sensitive tree biomass and is by itself able to limit the pace of 'bush encroachment' (Scholes and Archer 1997; Baudena et al. 2010; Yatat et al. 2014) while non-sensitive tree biomass has a widely recongised depressive effect on grass biomass by shading (Scholes and Archer 1997; Scholes 2003; Abbadie et al. 2006; Yatat et al. 2014). This effect can become facilitative in the driest zones (Scholes and Archer 1997, Abbadie et al. 2006, p. 156, Moustakas et al. 2013).

As in many models (Van Langevelde et al. 2003; Accatino et al. 2010; De Michele et al. 2011), we further assume that large tree are largely immune to fire impact (Trollope and Trollope 1996; Hoffmann and Solbrig 2003; Staver et al. 2011) and therefore make most of fire insensitive tree biomass. Fire impact concentrates on grasses and on small trees and shrubs. Grasses are known to rapidly recover while small trees and shrubs constituted the most of fire sensitive tree biomass (see arguments and references in Yatat et al. (2014)). We also assume periodic fire events which is an approximation that improves analytical tractability and seems however reasonable. Moreover, in the contexts where fires are frequent (humid savannas), they generally occur in specific periods in the year (Jeffery et al. 2014), while in protected areas (mesic savannas) fires are often set in the first part of the dry season (Scholes and Walker 1993; Govender et al. 2006; Diouf et al. 2012). Furthermore, most of available

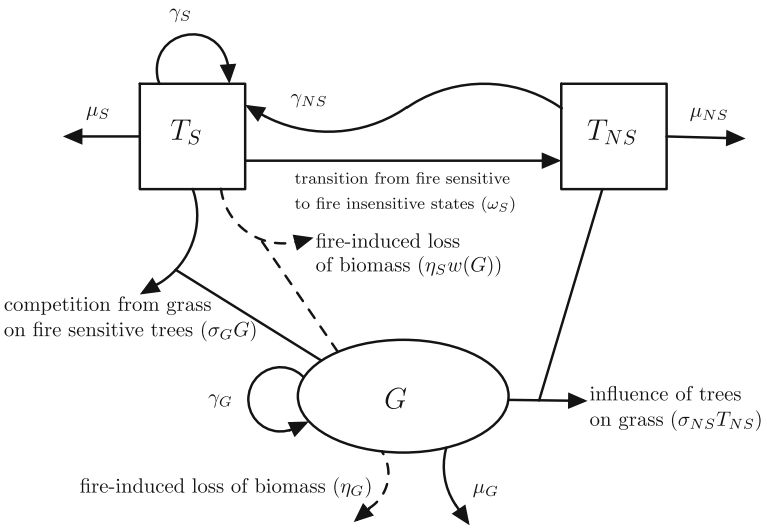

Fig. 1 Compartmental diagram of the size structured tree–grass interactions model in savanna. *Symbols* γ and μ express biomass growth and decay, respectively

data on fire occurrences are given in terms of fire-return time or fire period (Scholes and Archer 1997; Van Langevelde et al. 2003; Van Wilgen et al. 2004; Abbadie et al. 2006; Sankaran et al. 2008; Accatino et al. 2010; Calabrese et al. 2010; Staver and Bond 2014). Additionally, we model the fire intensity and ensuing impact on sensitive woody plants by a non-linear increasing and bounded function of grass biomass $w(G)$ (see also Staver et al. 2011; Yatat et al. 2014; Tchuinté et al. 2014).

The following diagram summarizes the relationship between the three compartments of vegetation (Fig. 1).

Therefore, based on these ecological premises, and taking into account the effect of fire as pulse-like phenomena, we propose a model for the savanna vegetation dynamics which is an extension of the continuous fire model of asymmetric tree–grass competition (COFAC) formulated in Yatat et al. (2014). The impulsive fire model of asymmetric tree–grass competition (IFAC) is given by

$$\begin{cases} \dfrac{dT_S}{dt} &= (\gamma_S T_S + \gamma_{NS} T_{NS})\left(1 - \dfrac{T_S + T_{NS}}{K_T}\right) - T_S(\mu_S + \omega_S + \sigma_G G), \\ \dfrac{dT_{NS}}{dt} &= \omega_S T_S - \mu_{NS} T_{NS}, \quad t \neq t_k \\ \dfrac{dG}{dt} &= \gamma_G \left(1 - \dfrac{G}{K_G}\right) G - (\sigma_{NS} T_{NS} + \mu_G) G, \end{cases} \tag{1}$$

$$\begin{cases} T_S(t_k^+) &= (1 - \eta_S w(G(t_k)))T_S(t_k), \\ T_{NS}(t_k^+) &= T_{NS}(t_k), \quad t = t_k, \quad t_{k+1} = t_k + \tau, \quad k = 1, 2, \ldots \\ G(t_k^+) &= (1 - \eta_G) G(t_k), \end{cases} \tag{2}$$

with

$$0 \leq T_S(0) = T_{S_0}, \quad 0 \leq T_{NS}(0) = T_{NS_0} \leq K_T, \quad 0 \leq G(0) = G_0, \tag{3}$$

where

- K_T, K_G (in tons per hectare, $t.ha^{-1}$) is the carrying capacity for tree and grass biomass, respectively.
- γ_{NS} (in yr^{-1}) expresses the rate at which sensitive tree biomass is produced from non-sensitive tree biomass (via seed production and successful germination) while γ_S (in yr^{-1}) stands as the intrinsic growth rate of sensitive tree biomass.
- γ_G (in yr^{-1}) denotes the intrinsic growth rate of grass biomass.
- μ_S (in yr^{-1}) is an additional death rate of sensitive tree biomass due to external disturbances such as human activities and herbivory.
- μ_{NS} (in yr^{-1}) is the death rate of non-sensitive tree biomass either natural or induced by human disturbance (e.g. wood-cutting).
- τ (in yr) is the fire-return time and $\tau = \dfrac{1}{f}$ where f (in yr^{-1}) is the fire frequency.
- μ_G (in yr^{-1}) is an additional death rate of grass biomass due to factors including human activities and herbivory.
- $\dfrac{1}{\omega_S}$ (in yr) is the average time that sensitive tree biomass takes to become non-sensitive to fire.

- σ_G expresses the asymmetric competition exerted by grass biomass on sensitive tree biomass (shading and root competition for nutrients, in $ha.t^{-1}.yr^{-1}$).
- σ_{NS} expresses the asymmetric interaction (competition and/or facilitation) of non-sensitive tree biomass on grass biomass (shading and competition for nutrients, in $ha.t^{-1}.yr^{-1}$).
- η_S is the proportion of fire sensitive tree biomass that is consumed by a fire event of a certain intensity (expressed by $w(G)$).
- η_G is the proportion of grass biomass that is consumed by fire.

We further assume that

$$\gamma_{NS} \geq \mu_{NS} \quad \text{and} \quad \gamma_S \geq \mu_S. \tag{4}$$

Condition (4) means that vegetation is here supposed to be always stable against desert for simplicity but with no loss of generality with respect to the potential of the model to describe savanna to desert transitions.

The structure of the IFAC calls for some remarks: first, we model the asymmetric effect of non-sensitive tree biomass onto grass biomass as a term affecting the production to mortality balance of the grass stratum (i.e. $\sigma_{NS}T_{NS}$). This choice is in agreement with the models of Tilman (1994), Accatino et al. (2010) and De Michele et al. (2011). Nevertheless, these authors (Tilman 1994; Accatino et al. 2010; De Michele et al. 2011) additionally introduced the feed-back into the logistic saturation, but such a position is mainly motivated by the fact that they modeled cover fractions (summing to one) of vegetation components instead of biomasses. Note that σ_{NS} will be generally positive (depressing effect) but may be negative (facilitation) in arid situations (Belsky et al. 1989; Belsky 1994; Weltzin and Coughenour 1990; Abbadie et al. 2006; Moustakas et al. 2013). Second, saturation of grass biomass is modeled with respect to K_G (t/ha) which will be equated in each of the main ecological zones (see Sect. 4) as the maximal standing crop value of a pure stand of grasses. Similarly, K_T can be considered as the maximal biomass reached in each zone by a woody stand that freely developed up to saturation. This will correspond to a wet forest and a dry forest in the humid and mesic zones, respectively. In the arid zone, there is ample evidence that tree-tree interactions for limiting soil resources often preclude a continuous woody cover (Sankaran et al. 2005, Deblauwe et al. 2008) and the saturation value, K_T, is likely to encompass various physiognomies. K_T integrates both sensitive and non-sensitive woody individuals but for obvious reasons, the non-sensitive individuals which are the tallest ones are expected to account for most of the corresponding biomass. The saturation effect is modeled as depressing the recruitment of small sized individuals (as universally observed, for instance, in a forest of closed canopy), and is therefore integrated in the equation depicting the dynamics of T_S. We show here-below that it is sufficient to also bound the value of T_{NS}.

For reader's convenience, let us recall that the COFAC (see Yatat et al. (2014)) and the IFAC differ by how fire events are modeled. Specifically, in the COFAC, fire events are time-continuous forcing while in the IFAC, fire events are pulse phenomena. As in Tchuinté et al. (2014) and Yatat et al. (2014), one can choose a generic sigmoidal function to model the fire intensity (see also Staver et al. (2011)). A typical choice could be

$$w(G) = \frac{G^\alpha}{G^\alpha + g_0^\alpha}, \tag{5}$$

where $G0 = g_0^\alpha$ is the value of grass biomass at which fire intensity reaches its half saturation (g_0 in tons per hectare, $t.ha^{-1}$) and $\alpha \in \mathbb{N}^*$. In the rest of the paper, we consider $\alpha = 2$.

3 Mathematical analysis and ecological interpretation of thresholds

3.1 Existence, positivity and boundedness of solutions

The right-hand side of system (1, 2) is locally lipschitz continuous on $\mathbb{R}^3$. Thus, using a classic existence theorem (Theorem 1.1, p. 3 in Bainov and Simeonov (1995)), there exist $\beta > 0$ and a unique solution defined from $(0, \beta) \longrightarrow \mathbb{R}^3$ for system (1–3).

System (1, 2) is designed to model tree–grass interactions in savanna ecosystems. Thus, it is important that its solutions remain positive and bounded such that our system is biologically well posed.

Lemma 1 (i) *The positive orthant $\mathbb{R}^3_+$ is a positively invariant region for the system (1)–(2).*

(ii) *The set Ω defined by*

$$\begin{aligned}\Omega \ &= \Big\{(T_S; T_{NS}; G) \in \mathbb{R}^3_+ \mid 0 \le T_S + T_{NS} \\ &\le \max\left\{K_T, \frac{\gamma_{NS} - \mu_{NS}}{\gamma_S} K_T, \frac{\gamma_S - \mu_S}{\gamma_{NS}} K_T\right\}; 0 \le G \le K_G\Big\}\end{aligned}$$

is an invariant and absorbing region for system (1–3).

Proof (See Appendix 7). □

In other words, from the set Ω we deduce that both woody and grassy biomasses remain positive and bounded. The overall woody biomass is bounded due to the first equation expressing the dynamics of fire sensitive tree biomass even though K_T does not appear in the dynamics of non-sensitive trees biomass (i.e. second equation). For this reason, mathematically, our system is a dissipative system (Hale 1988).

Remark 1 We further deduce from Lemma 1 that the aforementioned local solution of system (1–3) is a global solution i.e. defined on $[0, +\infty)$.

3.2 Trivial and semitrivial solutions

It is obvious that system (1, 2) has always a desert equilibrium $E_0 = (0, 0, 0)$.

3.2.1 The positive grassland periodic solution: existence and local stability

Let us consider the following thresholds:

$$\mathcal{R}_G^0 = \frac{\gamma_G}{\mu_G}, \qquad \mu_G > 0, \tag{6}$$

and

$$\rho_G^0 = \begin{cases} (1-\eta_G)\exp\left(\mu_G\left(\mathcal{R}_G^0 - 1\right)\tau\right), & \mu_G > 0, \\ (1-\eta_G)\exp\left(\gamma_G\tau\right), & \mu_G = 0. \end{cases} \tag{7}$$

Assume that $\mathcal{R}_G^0 > 1$, we have the following result (see also Dai et al. (2012))

Lemma 2 *When $\rho_G^0 > 1$, system (1, 2) has a positive grassland periodic solution $E_G = (0, 0, G^*(t))$, where*

$$G^*(t) = \begin{cases} \dfrac{K_G\left(1-\dfrac{1}{\mathcal{R}_G^0}\right)\left(\rho_G^0 - 1\right)}{(\rho_G^0 - 1) + \eta_G e^{-\mu_G(\mathcal{R}_G^0-1)(t-(n+1)\tau)}}, & \mu_G > 0, \\ & n\tau \le t < (n+1)\tau, \\ \dfrac{K_G\left(\rho_G^0 - 1\right)}{(\rho_G^0 - 1) + \eta_G e^{-\gamma_G(t-(n+1)\tau)}}, & \mu_G = 0. \end{cases} \tag{8}$$

Remark 2 (Thresholds interpretation)

- $\mathcal{R}_G^0$ is the average amount of biomass produced by a unit of grass biomass during its whole lifespan in absence of fires and depressing effect from non-sensitive tree biomass but subject to additional mortality caused by human activities or by herbivory.
- ρ_G^0 embodies the residual amount of grass biomass at any time-period that fires occur, from the grass biomass produced per unit of grass biomass.

Remark 3 An obvious computation leads to:

$$\begin{array}{ll} \mathcal{R}_G^0 < 1 \implies \rho_G^0 < 1, & \\ \rho_G^0 > 1 \iff \eta_G < 1 - \exp(-\mu_G(\mathcal{R}_G^0 - 1)\tau), & \mu_G > 0, \\ \rho_G^0 > 1 \iff \eta_G < 1 - \exp(-\gamma_G\tau), & \mu_G = 0. \end{array} \tag{9}$$

Let us state the following lemma which will be helpful for the sequel

Lemma 3 *When $\rho_G^0 > 1$,*

$$\begin{aligned} G_{int} &:= \frac{1}{\tau}\int_{n\tau}^{(n+1)\tau} G^*(s)ds = \frac{1}{\tau}\frac{K_G}{\gamma_G}\ln(\rho_G^0) \\ &= \frac{1}{\tau}\frac{K_G}{\gamma_G}\left(\ln(1-\eta_G) + (\gamma_G - \mu_G)\tau\right) > 0. \end{aligned} \tag{10}$$

Now we turn to look for local stability of that previous positive and periodic grassland solution. For that purpose, we will use the small perturbation technique and the Floquet theory (Hale 1980; D'Onofrio 2002; Chen et al. 2009), i.e. we will find conditions under which all the Floquet multipliers of the positive and periodic grassland solution have their absolute value less than unity or equal to unity (Hale 1980; D'Onofrio 2002; Chen et al. 2009).

Let

$$\begin{aligned}\mathcal{R}_G^T &= \frac{\gamma_S\mu_{NS}+\omega_S\gamma_{NS}}{\mu_{NS}(\mu_S+\omega_S)+\mu_{NS}\sigma_G G_{int}},\\ &= \frac{\gamma_S\mu_{NS}+\omega_S\gamma_{NS}}{\mu_{NS}(\mu_S+\omega_S)+\dfrac{\mu_{NS}\sigma_G}{\tau}\dfrac{K_G}{\gamma_G}\left(\ln(1-\eta_G)+(\gamma_G-\mu_G)\tau\right)},\\ \mathcal{A} &= \gamma_S\tau\left(1-\frac{1}{\mathcal{R}}\right),\end{aligned} \tag{11}$$

where

$$\mathcal{R} = \frac{\gamma_S}{\mu_S+\omega_S+\mu_{NS}+\sigma_G G_{int}}$$

and

$$\mathcal{B} = \tau^2\mu_{NS}\left(\mu_S+\omega_S+\sigma_G G_{int}\right)\left(1-\mathcal{R}_G^T\right).$$

Moreover, let λ_1, λ_2 be the roots of

$$\mathcal{P}(\lambda) = \lambda^2 - \mathcal{A}\lambda + \mathcal{B}$$

and

$$\rho_T = \max\{(1-\eta_S w(G^*(\tau)))e^{\lambda_1},\ e^{\lambda_2}\}. \tag{12}$$

The following result holds for system (1, 2).

Lemma 4 (Local stability of the grassland periodic solution E_G) *Suppose that the grassland periodic solution (E_G) exists i.e. $\mathcal{R}_G^0 > 1$ and $\rho_G^0 > 1$. Moreover,*

- *if $\mathcal{R}_G^T < 1$ then, E_G is locally asymptotically stable,*
- *if ($\mathcal{R}_G^T > 1$ and $\rho_T < 1$) then, E_G is locally asymptotically stable,*
- *if ($\mathcal{R}_G^T > 1$ and $\rho_T = 1$) then, E_G is locally stable.*
- *if ($\mathcal{R}_G^T > 1$ and $\rho_T > 1$) then, E_G is unstable.*

Proof (See Appendix 8).

Remark 4 (*Thresholds interpretation*) In the sequel, we provide approximative thresholds interpretation in order to favor an intuitive ecological comprehension of our results.

- $\mathcal{R}_G^T$ is the sum of the average amount of biomass produced by a sensitive/young plant competing with grass between two successive fires, and the average amount of biomass produced by a mature plant multiplied by the proportion of young plants biomass which reach the mature stage.
- ρ_T embodies both the residual non-sensitive trees biomass after each periodic fire events and the reduction of sensitive tree biomass due to competition with grass biomass.
  Moreover, since $\mathcal{R} < \mathcal{R}_G^T$, after a direct computation one has

$$\sigma_G < \frac{1}{G_{int}} \left(\gamma_S - (\mu_S + \omega_S + \mu_{NS})\right) \Longrightarrow \rho_T > 1. \tag{13}$$

  Therefore, it clearly appears following relation (13) that the grass biomass vs. sensitive tree biomass competition parameter σ_G is a bifurcation parameter for the IFAC that embodies the stability/instability of the grassland periodic solution (i.e. E_G).

3.2.2 The positive forest equilibrium: existence and local stability

Let

$$\mathcal{R}_T^0 = \frac{\gamma_S \mu_{NS} + \gamma_{NS} \omega_S}{\mu_{NS}(\mu_S + \omega_S)}. \tag{14}$$

The next result follows from Proposition 1 in Yatat et al. (2014).

Lemma 5 *If $\mathcal{R}_T^0 > 1$ then system (1, 2) has a positive forest equilibrium $E_T = (\bar{T}_S, \bar{T}_{NS}, 0)$, where*

$$\begin{aligned} \bar{T}_S &= \frac{K_T \mu_{NS}}{\mu_{NS} + \omega_S} \left(1 - \frac{1}{\mathcal{R}_T^0}\right), \\ \bar{T}_{NS} &= \frac{\omega_S}{\mu_{NS}} \bar{T}_S = \frac{K_T \omega_S}{\mu_{NS} + \omega_S} \left(1 - \frac{1}{\mathcal{R}_T^0}\right). \end{aligned} \tag{15}$$

As previously we are checking for local stability of the positive forest equilibrium. Let

$$\begin{aligned} \mathcal{R}_T^G &= \frac{\gamma_G}{\mu_G + \sigma_{NS} \bar{T}_{NS}}, \\ \rho_T^G &= (1 - \eta_G) \exp\left(\gamma_G \left(1 - \frac{1}{\mathcal{R}_T^G}\right) \tau\right). \end{aligned} \tag{16}$$

Using the same approach as in the proof of Lemma 4, we derive the following result.

Lemma 6 (Local stability of the forest equilibrium E_T) *Suppose that the forest equilibrium (E_T) exists, i.e. $\mathcal{R}_T^0 > 1$. Moreover,*

- *if $\mathcal{R}_T^G \leq 1$ then, E_T is locally asymptotically stable,*

- *if* $(\mathcal{R}_T^G > 1$ *and* $\rho_T^G < 1)$ *then,* E_T *is locally asymptotically stable,*
- *if* $(\mathcal{R}_T^G > 1$ *and* $\rho_T^G = 1)$ *then,* E_T *is locally stable .*
- *if* $(\mathcal{R}_T^G > 1$ *and* $\rho_T^G > 1)$ *then,* E_T *is unstable.*

Remark 5 (*Thresholds interpretation*) In the sequel, we provide approximative interpretation of the aforementioned thresholds.

- $\mathcal{R}_T^0$ is the sum of the average amount of biomass produced by a sensitive/young plant, without fires and competition from grass biomass, plus the average amount of biomass produced by a mature plant multiplied by the proportion of young plants biomass which reach the mature stage.
  We may note here that this threshold only depends on the parameters ruling the dynamics of the woody biomass.
- $\mathcal{R}_T^G$ is the average biomass produced by a unit of grass biomass during its whole lifespan free of fires but experiencing competition from non-sensitive tree biomass.
- ρ_T^G embodies both the residual grass biomass after a fire event and the biomass subjected to the depression by competition from non-sensitive tree biomass. One should also note that, when $\mathcal{R}_T^G > 1$, one has

$$\begin{aligned}\rho_T^G \leq 1 &\Longleftrightarrow \eta_G \geq 1 - \frac{1}{\exp\left(\gamma_G\left(1-\frac{1}{\mathcal{R}_T^G}\right)\tau\right)}\\ &\Longleftrightarrow \tau \leq -\frac{\ln(1-\eta_G)}{\gamma_G\left(1-\frac{1}{\mathcal{R}_T^G}\right)}\\ &\Longleftrightarrow \frac{1}{\overline{T}_{NS}}\left(\gamma_G - \mu_G + \frac{\ln(1-\eta_G)}{\tau}\right) \leq \sigma_{NS}. \qquad (17)\end{aligned}$$

  Therefore we can deduce three major observations.

  (i) Firstly, if the fires period τ is small (i.e. the fires frequency f is high) then $1 - \frac{1}{\exp\left(\gamma_G\left(1-\frac{1}{\mathcal{R}_T^G}\right)\tau\right)}$ is small and one can have $\rho_T^G \leq 1$ for small values of η_G. In other words, this means that despite frequent fire events, trees can outcompete grasses. It results that the forest state is stable under frequent fires due to the suppression of grass production under dense cover or one can observe a multy-stability involving forest state. This phenomenon has been observed in a wet tropical area in Gabon where dense forest and savanna of very low tree biomass co-occur within the same landscape (Jeffery et al. 2014).

  (ii) Secondly, if the fires period τ is large (i.e. the fires frequency f is small) then

$$1 - \frac{1}{\exp\left(\gamma_G\left(1-\frac{1}{\mathcal{R}_T^G}\right)\tau\right)} = 1 - \varepsilon,$$

where $0 < \varepsilon << 1$. Thus, following (17), $\rho_T^G \leq 1$ requires to have a large destruction of grass biomass (more than 99 %). This is ecologically not possible according to the fact that a part of the grass biomass like roots and even the bottom of the tufts, cannot burn. Therefore, in case of large fires period, having $\rho_T^G \leq 1$ may likely correspond to a decrease of $\mathcal{R}_T^G$ (i.e. an increase of σ_{NS}).

(iii) It is easily deduced from relation (17) that the fire-return time τ and the non-sensitive tree biomass vs. grass biomass competition/facilitation parameter σ_{NS} are bifurcation parameters for the IFAC that embody stability/instability of the forest equilibrium (i.e. E_T).

Remark 6 A direct comparison leads to:

1. $\mathcal{R}_G^T < \mathcal{R}_T^0$
2. $\mathcal{R}_G^0 < 1 \Longrightarrow \mathcal{R}_T^G < 1, \quad \mu_G > 0.$

3.2.3 Global stability of trivial equilibrium (desert) and semi-trivial solutions (grassland periodic solution and the forest equilibrium)

Here, we state a result concerning the global stability of the desert equilibrium, the forest equilibrium and a result concerning the global stability of the grassland periodic solution. Using the thresholds defined in (6), (7) and (14), we have the following

Theorem 1 • *Case 1:* $\mu_G > 0$.

1. *If* $\mathcal{R}_T^0 < 1$ *and* $\mathcal{R}_G^0 < 1$ *then the desert equilibrium* $E_0 = (0, 0, 0)$ *is globally asymptotically stable (GAS).*
2. *If* $\mathcal{R}_T^0 > 1$ *and* $\mathcal{R}_G^0 < 1$ *then the forest equilibrium* $E_T = (\bar{T}_S, \bar{T}_{NS}, 0)$*, where* $(\bar{T}_S, \bar{T}_{NS})$ *are given in (15), is globally asymptotically stable.*
3. *If* $\mathcal{R}_T^0 < 1$, $\mathcal{R}_G^0 > 1$ *and* $\rho_G^0 < 1$ *then the desert equilibrium* $E_0 = (0, 0, 0)$ *is globally asymptotically stable.*
4. *If* $\mathcal{R}_T^0 < 1$, $\mathcal{R}_G^0 > 1$ *and* $\rho_G^0 > 1$ *then the grassland periodic solution* $E_G = (0, 0, G^*(t))$*, where* $G^*(t)$ *is given by (8), is globally asymptotically stable.*

• *Case 2:* $\mu_G = 0$.

1. *If* $\mathcal{R}_T^0 < 1$ *and* $\rho_G^0 < 1$ *then the desert equilibrium* $E_0 = (0, 0, 0)$ *is globally asymptotically stable.*
2. *If* $\mathcal{R}_T^0 < 1$ *and* $\rho_G^0 > 1$ *then the grassland periodic solution* $E_G = (0, 0, G^*(t))$*, where* $G^*(t)$ *is given by (8), is globally asymptotically stable.*
3. *If* $\mathcal{R}_T^0 > 1$ *and* $\rho_G^0 < 1$ *then the forest equilibrium* $E_T = (\bar{T}_S, \bar{T}_{NS}, 0)$*, where* $(\bar{T}_S, \bar{T}_{NS})$ *are given in (15), is globally asymptotically stable.*

Proof (See Appendix 9). □

Remark 7 (*A comparison IFAC vs. COFAC*) In Yatat et al. (2014), we found the following threshold parameters:

$$\mathcal{R}_1^{\overline{G}} = \frac{\gamma_S \mu_{NS} + \gamma_{NS} \omega_S}{\mu_{NS}(\mu_S + \omega_S + \sigma_G \overline{G} + f \eta_S w(\overline{G}))}, \quad \text{where} \quad \overline{G} = K_G \left(1 - \frac{f\eta_G + \mu_G}{\gamma_G}\right),$$
$$\mathcal{R}_2^{\overline{T}_{NS}} = \frac{\gamma_G}{f\eta_G + \mu_G + \sigma_{NS} \overline{T}_{NS}}, \quad \text{where} \quad \overline{T}_{NS} \quad \text{is defined in (15).} \tag{18}$$

Straightforward computations lead to,

$$\mathcal{R}_1^{\overline{G}} < \mathcal{R}_G^T \quad \text{and} \quad \mathcal{R}_2^{\overline{T}_{NS}} < \mathcal{R}_T^G.$$

According to the previous results, we deduce the following:

1. If $\mathcal{R}_1^{\overline{G}} < \mathcal{R}_G^T < 1$ then grassland is locally asymptotically stable (LAS) for both IFAC and COFAC.
2. If $\mathcal{R}_1^{\overline{G}} < 1 < \mathcal{R}_G^T$ then grassland is LAS for the COFAC. But, depending on ρ_T, grassland can be either stable or unstable for the IFAC. However, for the IFAC, in the case that grassland is unstable, forest and/or savanna can be LAS.
3. If $1 < \mathcal{R}_1^{\overline{G}} < \mathcal{R}_G^T$ then grassland is unstable for the COFAC. Nonetheless, depending on ρ_T grassland can be either stable or unstable for the IFAC. Moreover, for the IFAC, when grassland is unstable, forest and/or savanna can be LAS.
4. If $\mathcal{R}_2^{\overline{T}_{NS}} < \mathcal{R}_T^G < 1$ then forest is LAS for both IFAC and COFAC.
5. If $\mathcal{R}_2^{\overline{T}_{NS}} < 1 < \mathcal{R}_T^G$ then forest is LAS for the COFAC and depending on ρ_T^G forest can be either stable or unstable for the IFAC. Moreover, with respect to the IFAC, in the case that forest is unstable, grassland and/or savanna can be LAS.
6. If $1 < \mathcal{R}_2^{\overline{T}_{NS}} < \mathcal{R}_T^G$ then forest is unstable for the COFAC. Nonetheless, depending on ρ_T^G forest can be either stable or unstable for the IFAC. With respect to the IFAC, when forest is unstable, grassland and/or savanna can be LAS.

In cases 1 and 4 the COFAC and the IFAC have the same qualitative behavior. In case 2 grassland is stable for the COFAC while it is either stable or unstable with the IFAC. Similarly, in case 5 forest is stable for the COFAC while it is either stable or unstable with the IFAC. Thus, the IFAC provides more diversified outcomes (see for instance Fig. 10, p. 33 and Fig. 13, p. 35 that illustrate some contrasting behaviors between the COFAC and the IFAC models). Theoretically, if we suppose that there exist some environmental settings that preclude grassland (resp. forest) state, and that the COFAC is in case 2 (resp. case 5) then, systematically, the COFAC will display spurious abrupt transitions while the IFAC could be more realistic in the sense that spurious shift from grassland to forest is not to be automatically expected for minor parameter changes. Finally, case 3 (resp. 6) suggests that grassland (resp. forest) is unstable for the COFAC which therefore prevents bistability situations involving these solutions (forest and grassland) or involving savanna plus one of them. In other words, even if environmental conditions in real-world situations strongly suggest bistability involving forest and grassland (as in Favier et al. (2012)), the COFAC will not render it and converge to case 3 or 6 whatever the parameters that may be chosen. IFAC is however able to render forest-grassland bistability as illustrated in Fig. 13, p. 35 for reasonable parameter values referring to a humid area of high grass production. Indeed mosaics of strong contrast between low woody biomass (virtually grasslands) and forests are a conspicuous, yet recurrent feature of transition landscapes under rainfall that can sustain continuous forest cover (Menaut 1983).

3.3 Existence of a positive and periodic tree–grass solution

Now, we reach the position to find at least one non-trivial positive and periodic solution of system (1, 2). We will use the approach developed by Gaines and Mawhin (1977).

Before we give the main result of this section, we recall useful inequalities according to the thresholds defined in (6) and (7)

1. If $\mathcal{R}_G^0 < 1$ then $\rho_G^0 < 1$.
2. $\rho_G^0 > 1 \Longleftrightarrow (\gamma_G - \mu_G) + \dfrac{\ln(1-\eta_G)}{\tau} > 0.$

The following result holds for system (1, 2).

Theorem 2 (Existence of a positive and periodic savanna solution)

- *Case 1:* $\mu_G > 0$.
  If $\mathcal{R}_G^0 > 1$ *and* $\rho_G^0 > 1$ *then system (1, 2) has at least one positive* τ*-periodic solution.*
- *Case 2:* $\mu_G = 0$.
  If $\rho_G^0 > 1$ *then system (1, 2) has at least one positive* τ*-periodic solution.*

Proof (See Appendix 10). □

Remark 8 One should note that Theorem 2 provides only sufficient conditions to ensure existence of at least one positive τ-periodic solution of system (1, 2). Thus, following Theorem 2, existence of savanna solution relies on sufficient grass biomass production.

Remark 9 Note also that, the uniqueness of the positive savanna solution is an open problem. In the rest of the paper, we will assume that we only have one positive solution.

As previously we address the question of local asymptotic stability of the positive and periodic savanna solution $E_{TG} = (\tilde{T}_S(t), \tilde{T}_{NS}(t), \tilde{G}(t))$. Defining

$$\begin{aligned} T_S(t) &= x(t) + \tilde{T}_S(t), \\ T_{NS}(t) &= y(t) + \tilde{T}_{NS}(t), \\ G(t) &= z(t) + \tilde{G}(t), \end{aligned} \tag{19}$$

where $x(t)$, $y(t)$ and $z(t)$ are small perturbations and satisfy

$$\begin{pmatrix} x(t) \\ y(t) \\ z(t) \end{pmatrix} = \Phi(t) \begin{pmatrix} x(0) \\ y(0) \\ z(0) \end{pmatrix}, \tag{20}$$

where Φ is a fundamental matrix and satisfies

$$\frac{d\Phi(t)}{dt} = DF(\tilde{T}_S(t); \tilde{T}_{NS}(t); \tilde{G}(t))\Phi(t) = \begin{pmatrix} a^{(1)} & a^{(2)} & -\sigma_G \tilde{T}_S(t) \\ \omega_S & -\mu_{NS} & 0 \\ 0 & -\sigma_{NS}\tilde{G}(t) & a^{(3)} \end{pmatrix} \Phi(t) \tag{21}$$

with

$$
\begin{aligned}
a^{(1)} &= \gamma_S\left(1-\frac{2\tilde{T}_S(t)+\tilde{T}_{NS}(t)}{K_T}\right)-\frac{\gamma_{NS}}{K_T}\tilde{T}_{NS}(t)-\sigma_G\tilde{G}(t)-\mu_S-\omega_S,\\
a^{(2)} &= \gamma_{NS}\left(1-\frac{\tilde{T}_S(t)+2\tilde{T}_{NS}(t)}{K_T}\right)-\frac{\gamma_S}{K_T}\tilde{T}_S(t),\\
a^{(3)} &= \gamma_G\left(1-\frac{2\tilde{G}(t)}{K_G}\right)-\sigma_{NS}\tilde{T}_{NS}(t)-\mu_G
\end{aligned}
\tag{22}
$$

and $\Phi(0) = Id_{\mathbb{R}^3}$. Furthermore, the resetting of impulsive condition of system (1, 2) becomes,

$$
\begin{pmatrix} x(n\tau^+)\\ y(n\tau^+)\\ z(n\tau^+)\end{pmatrix} = \begin{pmatrix} 1-\eta_S w(\tilde{G}(\tau)) & 0 & -w'(\tilde{G}(\tau))\tilde{T}_S(\tau)\\ 0 & 1 & 0\\ 0 & 0 & 1-\eta_G\end{pmatrix}\begin{pmatrix} x(n\tau)\\ y(n\tau)\\ z(n\tau)\end{pmatrix}. \tag{23}
$$

A monodromy matrix $\mathbf{M}$ of system (1, 2), is:

$$
\mathbf{M} = \begin{pmatrix} 1-\eta_S w(\tilde{G}(\tau)) & 0 & -w'(\tilde{G}(\tau))\tilde{T}_S(\tau)\\ 0 & 1 & 0\\ 0 & 0 & 1-\eta_G\end{pmatrix}\Phi(\tau), \tag{24}
$$

with

$$
\Phi(t) \;=\; \exp\left(\int_0^t DF(\tilde{T}_S(s);\tilde{T}_{NS}(s);\tilde{G}(s))ds\right). \tag{25}
$$

Let defined ρ_{TG} such as

$$
\rho_{TG} = \max(|\lambda| \;:\; \lambda \in sp(\mathbf{M})), \tag{26}
$$

where the matrix $\mathbf{M}$ is defined in (24). Therefore, following the Floquet theorem (Hale 1980; D'Onofrio 2002; Chen et al. 2009) we deduce the following results

Lemma 7
- *If $\rho_{TG} < 1$ then the positive τ-periodic solution of system (1, 2) is locally asymptotically stable.*
- *If $\rho_{TG} = 1$ then the positive τ-periodic solution of system (1, 2) is locally stable.*
- *If $\rho_{TG} > 1$ then the positive τ-periodic solution of system (1, 2) is unstable.*

Unfortunately, expressions (24) and (25) don't allow an explicit computation of the eigenvalues of the monodromy matrix $\mathbf{M}$ and of the real ρ_{TG}. Therefore, the stability of the positive τ-periodic solution of system (1, 2) will be conjectured through numerical computation of the threshold ρ_{TG}.

3.4 Summary table of the IFAC qualitative analysis

Based on the above studies, we deduce the summary Table of the qualitative analysis of the IFAC. In Table 1, **G** stands for Globally Asymptotically Stable, **L** stands for Locally Asymptotically Stable, **NU** stands for Numerical Asymptotical Stability and the empty cell denotes either the instability/non existence of the corresponding solution or that the result does not depend on the corresponding threshold. For reader's convenience, we recall all thresholds defined previously:

$$
\begin{aligned}
\mathcal{R}_T^0 &= \frac{\gamma_S \mu_{NS} + \gamma_{NS}\omega_S}{\mu_{NS}(\mu_S + \omega_S)},\\
\mathcal{R}_G^0 &= \frac{\gamma_G}{\mu_G}, \qquad \text{when } \mu_G > 0\\
\rho_G^0 &= (1-\eta_G)\exp\left(\mu_G\left(\mathcal{R}_G^0 - 1\right)\tau\right),\\
\mathcal{R}_T^G &= \frac{\gamma_G}{\mu_G + \sigma_{NS}\bar{T}_{NS}}, \quad \text{where } \bar{T}_{NS} = \frac{K_T\omega_S}{\mu_{NS}+\omega_S}\left(1 - \frac{1}{\mathcal{R}_T^0}\right)\\
\rho_T^G &= (1-\eta_G)\exp\left(\gamma_G\left(1 - \frac{1}{\mathcal{R}_T^G}\right)\tau\right),\\
\mathcal{R}_G^T &= \frac{\gamma_S\mu_{NS} + \omega_S\gamma_{NS}}{\mu_{NS}(\mu_S+\omega_S) + \dfrac{\mu_{NS}\sigma_G}{\tau}\dfrac{K_G}{\gamma_G}\left(\ln(1-\eta_G) + (\gamma_G - \mu_G)\tau\right)}
\end{aligned}
\tag{27}
$$

Table 1 Summary table of the qualitative analysis of system (1, 2) when $\mu_G > 0$. NU: LAS for E_{TG} needs to be estimated numerically by using formula (26)

Thresholds							Solutions				
$\mathcal{R}_T^0$	$\mathcal{R}_G^0$	$\mathcal{R}_T^G$	ρ_G^0	ρ_T^G	$\mathcal{R}_G^T$	ρ_T	E_0	E_T	E_G	E_{TG}	Case
>1	>1	>1	>1	>1	>1	>1				NU	1
						≤ 1			**L**	NU	2
					<1				**L**	NU	3
				≤ 1	>1	>1		**L**		NU	4
						≤ 1		**L**	**L**	NU	5
					<1			**L**	**L**	NU	6
			<1					**L**		NU	7
		<1	>1		>1	>1		**L**		NU	8
						≤ 1		**L**	**L**	NU	9
					<1			**L**	**L**	NU	10
			<1					**L**		NU	11
	<1							**G**			12
<1	>1		>1						**G**		13
			<1				**G**				14
	<1						**G**				15

and ρ_T is defined in (12). In Table 1, we present qualitative results of system (1, 2) when $\mu_G > 0$. The case $\mu_G = 0$ can be deduced from Table 1 by deleting the column related to R_G^0.

Remark 10 A direct computation leads

$$\begin{aligned}\rho_T^G &= (1-\eta_G)\exp\left(\gamma_G\left(1-\frac{1}{\mathcal{R}_T^G}\right)\tau\right)\\ &= (1-\eta_G)\exp\left((\gamma_G-\mu_G-\sigma_{NS}\bar{T}_{NS})\tau\right)\\ &= (1-\eta_G)\exp\left(\mu_G(\mathcal{R}_G^0-1)\tau\right)\exp\left(-\sigma_{NS}\bar{T}_{NS}\tau\right)\\ \rho_T^G &= \rho_G^0\exp(-\tau\sigma_{NS}\bar{T}_{NS}).\end{aligned} \tag{28}$$

Therefore, according to (28), when $\mathcal{R}_T^0 > 1$ i.e. $\bar{T}_{NS} > 0$ then $\rho_T^G < \rho_G^0$.

In the sequel, we provide some numerical simulations in order to illustrate our theoretical results. To achieve that goal, first we will provide a suitable nonstandard numerical scheme which will be helpful for the numerical approximation of the IFAC solutions. Standard methods (such as Runge–Kutta or Euler methods) can sometimes present spurious behaviors which are not in adequacy with the system properties that they aim to approximate i.e., lead to negative solutions, exhibit numerical instabilities, or even converge to the wrong equilibrium for certain values of the time discretization or the model parameters (interested readers can also see Dumont et al. (2010); Dumont and Tchuenche (2012); Anguelov et al. (2012, 2013, 2014); Yatat et al. (2014) for motivations, details and explanations about nonstandard schemes). Secondly, we will focus on three ecological regions of the African continent that contrast in terms of biomass production conditions, namely a semi-arid, a mesic and a humid region, to discuss the IFAC outcomes with respect to published modelling results on savanna ecosystems (Mordelet and Menaut 1995; Accatino et al. 2010; Moustakas et al. 2013; February et al. 2013; Baudena et al. 2014).

4 Nonstandard scheme, parameter ranges and ecological zones of biomass production

4.1 A nonstandard scheme for the IFAC

The nonstandard numerical scheme proposed in this section is adapted from the nonstandard scheme proposed for the COFAC model in Yatat et al. (2014).

System (1) is discretized as follows:

$$\begin{cases} \dfrac{G^{k+1}-G^k}{\phi_G(h)} = \gamma_G\left(1-\dfrac{G^{k+1}}{K_G}\right)G^k - \sigma_{NS}T_{NS}^k G^{k+1} - \mu_G G^k, \\ \dfrac{T_{NS}^{k+1}-T_{NS}^k}{\phi(h)} = \omega_S T_S^k - \mu_{NS}T_{NS}^{k+1}, \\ \dfrac{T_S^{k+1}-T_S^k}{\phi(h)} = (\gamma_S - (\mu_S+\omega_S))T_S^k + \gamma_{NS}T_{NS}^{k+1} - \dfrac{\gamma_S}{K_T}T_S^k(T_S^{k+1}+T_{NS}^{k+1}) \\ \qquad\qquad -\dfrac{\gamma_{NS}}{K_T}T_{NS}^k T_{NS}^{k+1} - \left(\dfrac{\gamma_{NS}}{K_T}T_{NS}^k + \sigma_G G^k\right)T_S^{k+1}, \end{cases} \tag{29}$$

and the impulsive event (2) is discretized as follows:

$$\begin{cases} G_+^{k+1} = (1-\eta_G)G^{k+1} \\ T_{NS+}^{k+1} = T_{NS}^{k+1}, \\ T_{S+}^{k+1} = (1-\eta_S w(G^{k+1}))T_S^{k+1}, \end{cases} \tag{30}$$

where the denominator functions ϕ and ϕ_1 read as

$$\phi(h) = \frac{e^{Qh}-1}{Q}, \quad h>0, \tag{31}$$

with

$$Q = \max\left(\mu_{NS}, \gamma_S - (\mu_S+\omega_S)\right). \tag{32}$$

Using the fact that $\gamma_G - \mu_G = \mu_G(\mathcal{R}_G^0 - 1)$, we define

$$\phi_G(h) = \begin{cases} \dfrac{e^{\mu_G(\mathcal{R}_G^0-1)h}-1}{\mu_G(\mathcal{R}_G^0-1)}, & \mu_G > 0. \\ \dfrac{e^{\gamma_G h}-1}{\gamma_G}, & \mu_G = 0, \quad h>0. \end{cases} \tag{33}$$

This scheme is positively invariant and is qualitatively stable, which means that it has the same equilibria than system (1, 2), and the stability/instability properties of the equilibria are preserved, at least locally, whatever the stepsize $h > 0$ (Yatat et al. 2014).

4.2 Parameter ranges and ecological zones of biomass production

To provide relevant numerical simulations, one need to use ecologically meaningful parameter ranges and values. Thus, after extensive literature review, we reached the following parameter ranges (Table 2, p. 20).

We agree that, in the real world, fire is a stochastic phenomenon, and fire frequency or fire-return time thus generally experiences strong variations in a given location as

Table 2 Parameter ranges and values found in literature

Parameters	Values	References
K_T	10–120	Mermoz et al. (2014)
K_G	1–20	Penning de Vries and Djiteye (1982), Abbadie et al. (2006)
γ_G	$0.4^{(1)}$–$4.6^{(2)}$	$^{(1)}$ Penning de Vries and Djiteye (1982), $^{(2)}$ Menaut and César (1979)
$\gamma_S + \gamma_{NS}$	0.456–7.2	Breman and Kessler (1995)
μ_{NS}	0.03–0.3	Accatino et al. (2010)
	0.4	Van Langevelde et al. (2003)
μ_S	0–0.3	Van Langevelde et al. (2003)
μ_G	0–0.6	Van Langevelde et al. (2003)
η_G	$0.1^{(a)}$–$1^{(b)}$	$^{(a)}$ Van de Vijver et al. (1999)
		$^{(b)}$ Accatino et al. (2010)
	0.2–1	Abbadie et al. (2006)
η_S	0.02–0.6	Accatino et al. (2010)
	0.66	Reinterpretation of Gignoux (1994), Reinterpretation of Van Langevelde et al. (2003)
ω_S	0.05–0.2	Wakeling et al. (2011)

pointed out by Archibald et al. (2009). According to those authors such variation is particularly high in mesic savannas while the explanatory power of physical, climatic, and human drivers of fires is substantial yet limited (Archibald et al. 2009). However, in order to reach analytical results, we just consider average values of fire frequency or fire-return time without considering variability around the mean. The ranges of "central" values retained for each of the three ecological zones, as provided in Tables 3 and 4, p. 21, encompass the fire-return time values reported by Menaut and César (1979), Trollope (1984), Frost and Robertson (1985), Van Wilgen et al. (2004), Bond and Keeley (2005), Abbadie et al. (2006), Gignoux et al. (2009), Accatino et al. (2010), February et al. (2013) and Jeffery et al. (2014).

As stated previously, we will focus our numerical simulations on three ecological zones of the African continent.

Region 1 is an area with a relatively low mean annual rainfall (semi-arid region) where there is a low grass biomass production and therefore infrequent fires (Archibald et al. 2009). We consider such a region as qualitatively in agreement with the conditions described by Moro et al. (1997) (mean annual rainfall (MAR) of $259\,mm.yr^{-1}$), Smit and Rethman (2000) (MAR of $376\,mm.yr^{-1}$), February et al. (2013) (MAR of $547\,mm.yr^{-1}$) and Higgins et al. (1999) (MAR of $670\,mm.yr^{-1}$). Moreover, Frost and Robertson (1985) found that in these regions, the fire-return time is about five to fifty

Table 3 Average fire period (τ, in yr) ranges and values found in literature with respect of the mean annual rainfall (MAR)

	Ranges/values	References
Low MAR	5–50	Frost and Robertson (1985)
	4–8	Trollope (1984)
Intermediate MAR	3–5	February et al. (2013)
	5–7	Van Wilgen et al. (2004)
High MAR	0.5–3	Jeffery et al. (2014)
	0.5–2	Bond and Keeley (2005)
		Accatino et al. (2010)
	1–5	Abbadie et al. (2006)
	1	Menaut and César (1979)
		Gignoux et al. (2009)

Table 4 Parameter ranges in the three ecological regions

Parameter	Region 1	Region 2	Region 3	References
$\tau\ (yr)$	> 5	2–5	0.5–3	Menaut and César (1979), Frost and Robertson (1985), Van Wilgen et al. (2004), Bond and Keeley (2005), Abbadie et al. (2006), Gignoux et al. (2009), Accatino et al. (2010), Jeffery et al. (2014)
$K_T\ (t.ha^{-1})$	20–40	80–90	110–120	Mermoz et al. (2014)
$K_G\ (t.ha^{-1})$	1–5	5–10	10–20	Penning de Vries and Djiteye (1982), Abbadie et al. (2006)
$\gamma_G\ (yr^{-1})$	0.4–2	2–3.5	3.5–4.6	Menaut and César (1979), Penning de Vries and Djiteye (1982)
$\gamma_S\ (yr^{-1})$	0.2–0.8	0.2–1	1.5–2.7	Breman and Kessler (1995)
$\gamma_{NS}\ (yr^{-1})$	0.256–1.2	1.2–2.5	2.5–4.5	Breman and Kessler (1995)

years. Thus, we conclude on few fire occurrences (says one fire event every five years) if any and set the upper MAR boundary of this zone at about $650 mm.yr^{-1}$ which has also been proposed by Sankaran et al. (2005) as the limit between climate vs. disturbance control of woody cover.

Region 2 is an intermediate biomass production zone identified as a mesic area which broad features correspond to the contexts described by February et al. (2013) (MAR of $737 mm.yr^{-1}$) and Lehmann et al. (2008) (MAR of $1286 mm.yr^{-1}$). Moreover, Van Wilgen et al. (2004) found fire-return

intervals of five to seven years while February et al. (2013) found fire-return time of three to five years for similar areas. We further conclude that fire-return time is in order of three-five years, sometimes less.

Region 3 is a high biomass production zone with relatively high value of MAR. For this humid type of savanna we refer to studies such as Abbadie et al. (2006) (MAR of $1192\,mm.yr^{-1}$), Jeffery et al. (2014) (MAR of $1483\,mm.yr^{-1}$ with two rainy seasons). Moreover, Jeffery et al. (2014) observed annual fires in Region 3 (see also Menaut and César 1979; Gignoux et al. 2009) and even twice a year for regimes managed by local communities while Abbadie et al. (2006), p. 51, gave the range of 1–5 years for fire-return time. We therefore conclude that, in Region 3, fire-return time ranges from 0.5 to 3 years.

Our aim is to assess the different outcomes of the IFAC along with the influence of the variations of σ_G, σ_{NS} (for which there is no direct information in the published literature) and the fire period τ. From the available literature (see also Table 2, p. 20) and overall expert-based knowledge, we reach the following ranges for the other parameters as in Table 4, p. 21.

In addition, reinterpreting experiments that concern Region 1 and Region 2 as reported in February et al. (2013) we derived σ_G (in $ha.t^{-1}.yr^{-1}$): 0.1843–0.9984 for Region 1 and σ_G: 0.2470–1.6287 for Region 2. Moreover, several studies located under different rainfall compared grass production under and outside a tree crown. A synthesis was proposed by Mordelet & Le Roux (see Abbadie et al. (2006) p. 156) that emphasized that the relative production (within to outside) is a decreasing function along the rainfall gradient. We re-interpreted the results as to derive reasonable values for σ_{NS} in each of the three regions, using the subsequent reasoning.

Considering that the measurements were made, free of fires, in grass stands having reached the maximum standing crop, and letting G_u and G_o be the equilibrium values under and outside crown, respectively. We can write according to the model:

$$\begin{aligned} G_u &= K_G\left(1 - \frac{\mu_G + \sigma_{NS}\tilde{T}}{\gamma_G}\right) \\ G_o &= K_G\left(1 - \frac{\mu_G}{\gamma_G}\right). \end{aligned} \tag{34}$$

The ratio considered by Mordelet and Menaut (1995) (see also Abbadie et al. (2006) p. 156) is:

$$\delta_G = \frac{G_u}{G_o}, \tag{35}$$

i.e. the ratio of grass production under and outside a tree crown. Assuming $\mu_G = 0$, for the reported observational conditions, we can simplify as:

$$\delta_G = 1 - \frac{\sigma_{NS}\tilde{T}}{\gamma_G} \Longleftrightarrow \sigma_{NS} = \frac{(1-\delta_G)\gamma_G}{\tilde{T}}. \tag{36}$$

Table 5 Variation range of σ_{NS} in Region 1, Region 2 and Region 3 following re-interpretation of Mordelet & Le Roux results

	δ_G	γ_G	K_T	ε (min)	ε (max)	S	σ_{NS} (min)	σ_{NS} (max)
Region 1	1.58	0.6	30	0.4	0.75	1	−0.029	−0.0155
Region 2	1.25	2.8	85	0.2	0.67	1	−0.0412	−0.0123
	0.75						0.0123	0.0412
Region 3	0.75	4.2	115	0.1	0.15	1	0.0609	0.0913

$\tilde{T}$ is the woody biomass density to be computed at the scale of an isolated, full grown tree (having reached the maximal height considering the local climate) in any of the three regions.

We propose to relate $\tilde{T}$ to K_T as

$$\tilde{T} = \frac{\varepsilon \times K_T}{S},$$

where S is the woody cover characterizing the maximal density K_T and $\varepsilon \in]0, 1[$ is a coefficient expressing that an isolated tree has less influence on grass production than a complete, closed canopy stand corresponding to K_T.

We used the value of $\delta_G = 1.58$ (resp. 1.25 and 0.75, 0.75) of Mordelet and Menaut (1995) (see also Abbadie et al. (2006) p. 156) that corresponds to Region 1 (semi-arid region) (resp. Region 2, Region 3). Note that δ_G values above 1 express a facilitative effect of tree cover on grasses while values below correspond to a depressing effect. Using also the estimated values for K_T and γ_G, we deduce the ranges of variation of σ_{NS} (in ha.t^{-1}.yr^{-1}), summarized in Table 5, p. 23.

Note that the range of values for σ_{NS} is due to a large uncertainty on ε. Moreover as a straightforward consequence of the results of the reference study (Mordelet and Menaut 1995; Abbadie et al. 2006) σ_{NS} is likely to be negative in Region 1 where shading improves grass production, which is also in good agreement with results of Belsky et al. (1989); Belsky (1994), Weltzin and Coughenour (1990), Moustakas et al. (2013) and Barbier et al. (2008) (relating to the soil water budget).

5 Numerical simulations

As we stated previously, our aim is to illustrate the different outcomes of the IFAC and assess the influence of the variations of σ_G, σ_{NS} and the fire period τ. The proposed numerical simulations are of two kinds: phase diagrams (Figs. 3, 6, 7, 8, 9, 10, 12, 13) and level curves (Figs. 2, 4, 5, 11). Recall that, phase diagrams illustrate outcomes of the model for particular values of model parameters while level curves give the possibility to systematically simulate while letting a couple of parameters vary over their ranges of plausible values and therefore attenuate the consequence of the choice of particular values (e.g. τ, σ_G, σ_{NS}).

5.1 Results for Region 1

In semi-arid areas, the main mechanisms that govern the ecological processes of tree–grass interactions include

- **(M1)** water limitation on tree growth and, therefore, on woody cover (Sankaran et al. 2005; Baudena et al. 2014) and on grass biomass standing crop (K_G)
- **(M2)** tree–grass competition, which is an asymmetric competition on grass upon tree seedlings (February et al. 2013; Baudena et al. 2014)
- **(M3)** unfrequent fire may reduces woody cover and grass cover but grass biomass recover quickly after fire (Baudena et al. 2014) while low values of grass biomass limit the impact of competition on sensitive tree biomass.

Point **(M2)** suggests that the grass biomass vs. sensitive tree biomass competition parameter σ_G has relatively large values while point **(M1)** along with point **(M3)** suggest that woody cover is controlled principally by water availability and secondarily by unfrequent fires (Sankaran et al. 2005). Theoretically, if competition within life-forms is stronger that between life-forms, coexistence of woody and grassy biomasses is possible. Density and pattern of woody biomass distribution across savannas are likely governed by tree-tree interactions (Scholes and Archer 1997; Calabrese et al. 2010) which further impact grass biomass distribution.

The effect of scattered woody cover on grass biomass mainly results from reduced light availability and root competition for soil water (see Walker et al. 1981). Nevertheless, several references (Belsky et al. 1989; Belsky 1994; Weltzin and Coughenour 1990) also emphasized the facilitation role of scattered tree on grass biomass in East African semi-arid savannas. Indeed, compared with the open situation, the highest grass production was recorded under acacia and baobab trees (Belsky et al. 1989; Weltzin and Coughenour 1990; Mordelet and Menaut 1995), which are known to have a low light interception and only induce a slight limitation to photosynthesis while shading improves the water balance under the canopy (Barbier et al. (2008)). This finding can also be explained by the soil enrichment by nitrogen fixing species, like acacias trees which results in a yield increase. Therefore, in semi-arid areas the main ecological vegetation types that are observed depending on annual rainfall (which only varies tree/grass ratio) are savannas (Accatino et al. 2010; February et al. 2013; Baudena et al. 2014) and sometimes forest in the sense of low dry forest, and/or thickets (Walker et al. 1981; Couteron and Kokou 1997). The outcome of the IFAC in semi-arid areas is also in adequacy with this previous features. Indeed, let us consider the following table of parameter values (Table 6, p. 26).

For values in Table 6, we compute $\mathcal{R}_T^0 = 3.2222$, $\mathcal{R}_G^0 = 2$ and we derive Figs. 2 (p. 25) and 3 (p. 26).

In Fig. 3 we illustrate a transition from a forest state to a savanna state in Region 1 as the tree vs. grass facilitation parameter σ_{NS} increases. Indeed, with a low value of σ_{NS} that corresponds to a low level of facilitation effect, the forest equilibrium is stable (see panel (a), Fig. 3). Conversely, when the facilitation effect (including amelioration of microclimatic conditions, amelioration of ressource/nutrients availability, see also Belsky et al. (1989); Belsky (1994), Weltzin and Coughenour (1990), Scholes and Archer (1997), Abbadie et al. (2006), Moustakas et al. (2013)) increases, forest state

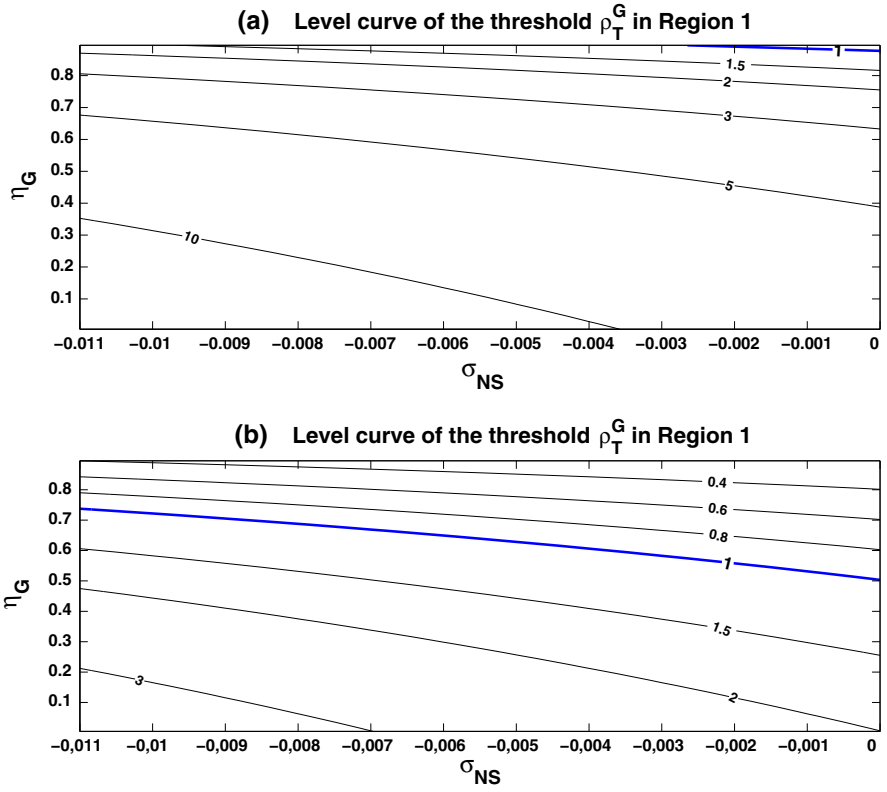

Fig. 2 Level curves of the threshold ρ_T^G illustrating that as η_G, μ_G and σ_{NS} increase, ρ_T^G decreases and consequently system (1, 2) is liable to move from a savanna/grassland state to a forest state or to a multistability involving the forest solution. Recall that the forest solution is stable (resp. unstable) whenever ρ_T^G is lower (resp. greater) than unity. In **a** $\mu_G = 0.3$, in **b** $\mu_G = 0.5$

is unstable while the savanna periodic solution is stable (see panel (b), Fig. 3, p. 26). Therefore, observed savanna-like vegetation formation in drier ecosystems can be explained by facilitative effects that may exist between tree and grass biomasses in such regions. Finally, based on our numerical simulations, we conjectured that panel (a) (see Fig. 3) depicts case 4 of Table 1 with savanna solution being unstable while panel (b) illustrates case 1.

Recall that according to relation (9),

$$\rho_G^0 > 1 \Longleftrightarrow \eta_G < \begin{cases} 0.8775 & \text{for } \mu_G = 0.3 \\ 0.5034 & \text{for } \mu_G = 0.5. \end{cases}$$

Moreover, together with our data estimation of σ_G and σ_{NS} in Region 1, we found that $\mathcal{R}_T^G > 1$. Setting $\mu_G = 0.3$, $\eta_G = 0.6$, and

- when $\sigma_G \in [0.1843, 0.92[$, we have $\rho_T > 1$
- when $\sigma_G \in [0.92, 0.95[$, we have $\mathcal{R}_G^T > 1$ and $\rho_T \leq 1$

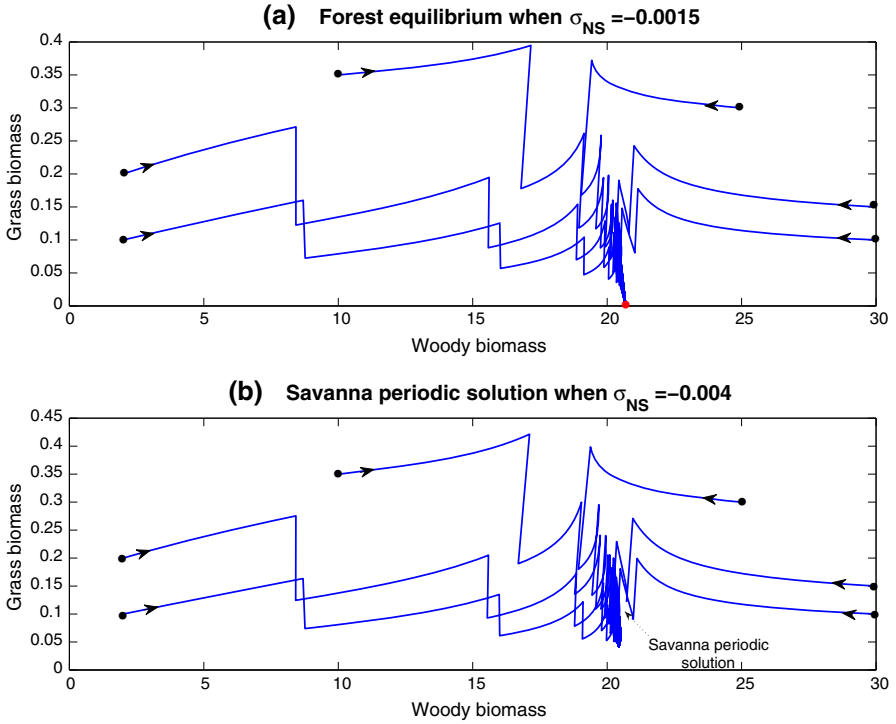

Fig. 3 Phase diagram of the IFAC illustrating a forest to savanna transition in Region 1 as the tree vs. grass facilitation parameter varies. In **a** with $\sigma_G = 0.1$, $\sigma_{NS} = -0.0015$, $\eta_G = 0.55$ and $\mu_G = 0.5$ the forest equilibrium (*red bullet*) is stable while in **b** with $\sigma_G = 0.1$, $\sigma_{NS} = -0.004$, $\eta_G = 0.55$ and $\mu_G = 0.5$, the savanna periodic solution is stable. Moreover, **a** illustrates case 4 of Table 1 with $\rho_T^G = 0.9885$ and the savanna solution being numerically unstable. Panel **b** illustrates case 1 of Table 1 with $\rho_{TG} = 0.9161$. The rest of the parameters are given in Table 6 (color figure online)

Table 6 Array of parameter' values for Region 1

$\tau = 7$, $K_T = 30$, $K_G = 2.5$,$G0 = 2$, $\sigma_G = 0.1$

γ_S	γ_{NS}	γ_G	μ_{NS}	ω_S	μ_S	η_S
0.3	1	0.6	0.15	0.1	0.2	0.5

– when $\sigma_G \in [0.95, 0.9984[$, we have $\mathcal{R}_G^T \leq 1$ and $\rho_T \leq 1$.

Finally, when $\mu_G = 0.5$ one gets $\rho_T > 1$. Therefore, Fig. 2, p. 25, together with the previous discussion on $\mathcal{R}_G^T$ and ρ_T illustrates case 1–case 7 of Table 1. Thus, when external disturbances (such as herbivory) on grass biomass are low and σ_G has relatively large values, $\rho_T \leq 1$ the IFAC predicts either a stable savanna state, a stable forest state, a stable grassland state or a multistability involving savanna and/or forest and/or grassland (see also case 1, case 2, case 3, case 4, case 5, case 6 and case 7 of Table 1). Furthermore, when external disturbances affecting the grass layer (embodied by μ_G) become more important, the grassland solution becomes unstable and the IFAC predicts either a stable savanna state, a stable forest state or a bistability involving savanna and foret states (see also case 1 and case 4 of Table 1). Consequently, one can

observe that the non-sensitive tree biomass vs. grass biomass interaction parameter σ_{NS} and the additional death rate of grass biomass due to external disturbances μ_G are likely to be influential on the IFAC outcomes in Region 1. Nevertheless, in the most arid part of Region 1 with a mean annual rainfall of 300–400 mm there is a wide array of references evidencing the probable bistability of desert (bare soil) and thickets (in the African Sahel) (see Couteron and Kokou 1997; Barbier et al. 2008; Lefever et al. 2009) or desert and grass (Namibia) (see Tschinkel 2012; Fernandez-Oto et al. 2014). However conditions leading to the desert state are not a focus of the present paper.

5.2 Results for Region 2

In Region 2 that corresponds to a mesic area, regulation of tree–grass interactions also include mechanisms **(M1)** and **(M2)** stated previously for semi-arid areas. In addition to **(M1)** and **(M2)**, fires are more frequent in mesic areas than in semi-arid areas since water availability favor grass biomass production which constitutes the fuel for fires (we denote this new mechanism **(M4)**). Grass-fire feedback (denoted mechanism **M4**) together with mechanisms **(M1)** and **(M2)**, maintain both forest and savanna occurrences in mesic areas (Baudena et al. 2014). Indeed, grasses benefit from the openness of the landscape after fires, since they recover faster than trees seedlings, thus determining a positive feedback mechanism that enhances savanna presence. The IFAC also predict a shift from a forest state to a savanna state as σ_{NS} decreases and/or when σ_G increases, which also agree with Baudena et al. (2014) results. Therefore,

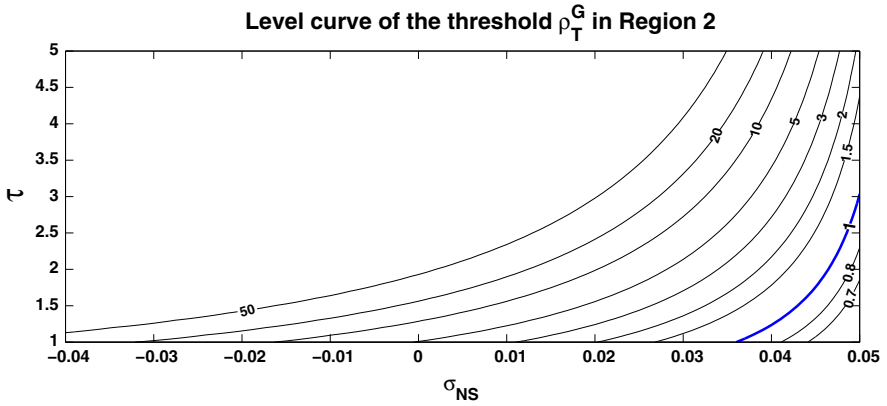

Fig. 4 Level curves of the threshold ρ_T^G illustrating that system (1, 2) is liable to move from a savanna/grassland state to a forest state or to a multistability involving the forest solution as a consequence of τ and σ_{NS} variations. Recall that the forest solution is stable (resp. unstable) whenever ρ_T^G is lower (resp. greater) than unity

Table 7 Array of parameter' values for Region 2

$K_T = 85$, $K_G = 7$, $\mu_G = 0.3$, $G0 = 2$

γ_S	γ_{NS}	γ_G	μ_{NS}	ω_S	η_S	η_G	μ_S
0.4	2	2.8	0.08	0.1	0.5	0.6	0.1

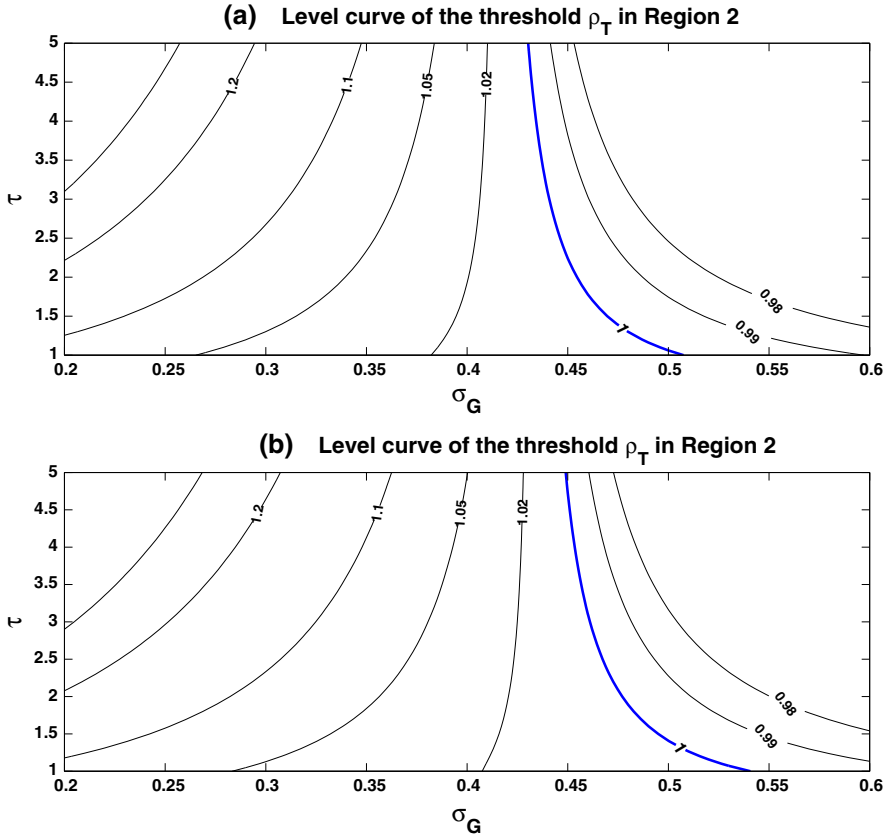

Fig. 5 Level curves of the threshold ρ_T illustrating that system (1, 2) is liable to move from a savanna/forest state to a grassland state or to a multistability involving the grassland solution in relation to τ and σ_G variations. Recall that the grassland solution is stable (resp. unstable) whenever ρ_T is lower (resp. greater) than unity. In **a** $\mu_G = 0.2$, in **b** $\mu_G = 0.3$

depending on σ_G and σ_{NS} variation in Region 2, savanna and forest vegetation types clearly appear as alternative stable states (see also Staver et al. 2011; Staver and Levin 2012).

Let us consider the following table of parameter values (Table 7, p. 27).

Using parameter values in Table 7, one has $\mathcal{R}_T^0 = 14.5$, $\mathcal{R}_G^0 = 14$ and we also derive Figs. 4 (p. 27), 5 (p. 28), 6 (p. 29), 7 (p. 30), 8 (p. 31) and 9 (p. 32).

Figure 6 illustrates the stability of the forest equilibrium (panel (a)) and the stability of the grassland periodic solution (panel (b)). Based on numerical computations we conjectured that, at least for Fig. 6, the savanna periodic solution is unstable. Finally, Fig. 6 also depicts cases 3 and 4 of Table 1.

Figure 7 illustrates a transition from a savanna state to a forest state while Fig. 8 illustrates a transition from a savanna state to a grassland state. Following our numerical simulations we further conjectured that the savanna periodic solution is unstable in panel (b) of both Figs. 7 and 8. Moreover, Fig. 7 illustrates cases 1 and 4 of Table 1 while Fig. 7 illustrates cases 1 and 2.

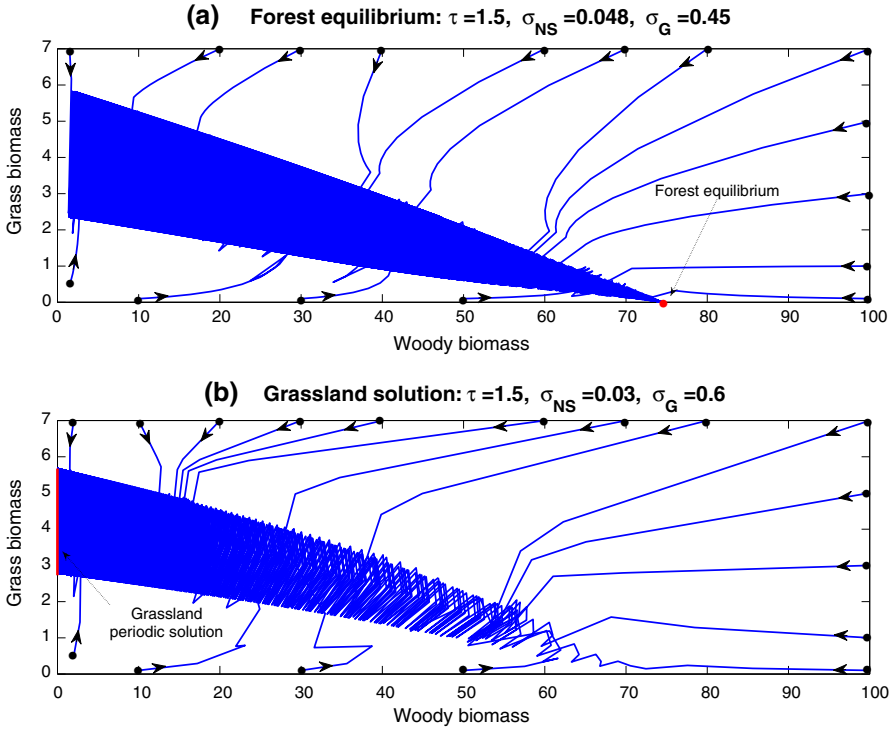

Fig. 6 Phase diagram of the IFAC illustrating a stable forest equilibrium (**a**, *red bullet*) and a stable grassland periodic solution (**b**, *red line*) with $\tau = 1.5$ and $K_T = 80$. Moreover, in **a**, $\sigma_G = 0.45$, $\sigma_{NS} = 0.048$ and it illustrates case 4 of Table 1 with $\rho_T^G = 0.8645$ and the savanna periodic solution being numerically unstable. In **b**, $\sigma_G = 0.6$, $\sigma_{NS} = 0.03$ and it illustrates case 3 of Table 1 with $\mathcal{R}_G^T = 0.9559$, $\rho_T = 0.9810$ and the savanna periodic solution being numerically unstable. The rest of the parameters are given in Table 7, p.27 (color figure online)

In Fig. 9 we illustrate a transition from a grassland state to a bistability situation involving grassland periodic solution and forest equilibrium. Recall that in bistability situation, the system convergence depends on initial data. Based on our numerical simulations, we conjectured that the savanna periodic solution is unstable in Fig. 9. Figure 9 also illustrates cases 2 and 5 of Table 1.

Since for parameter values in Table 7 one has $\mathcal{R}_G^0 > 1$ then,

$$\rho_G^0 > 1 \Longleftrightarrow \tau > \begin{cases} 0.3524 & \text{for } \mu_G = 0.2 \\ 0.3665 & \text{for } \mu_G = 0.3. \end{cases}$$

Moreover, for our estimation of σ_{NS} and σ_G one also has $\mathcal{R}_T^G > 1$ and $\mathcal{R}_G^T > 1$. Therefore, Figs. 4 and 5 illustrate, either case 1, case 2, case 3 or case 4 or case 5 in Table 1.

In summary, the parameters that are likely to be influential on the IFAC outcomes in Region 2 are the external disturbances on grass biomass parameter μ_G, the grass biomass vs. sensitive tree biomass parameter σ_G, the non-sensitive tree biomass vs. grass biomass interaction parameter σ_{NS}. In addition to that previous parameters, one

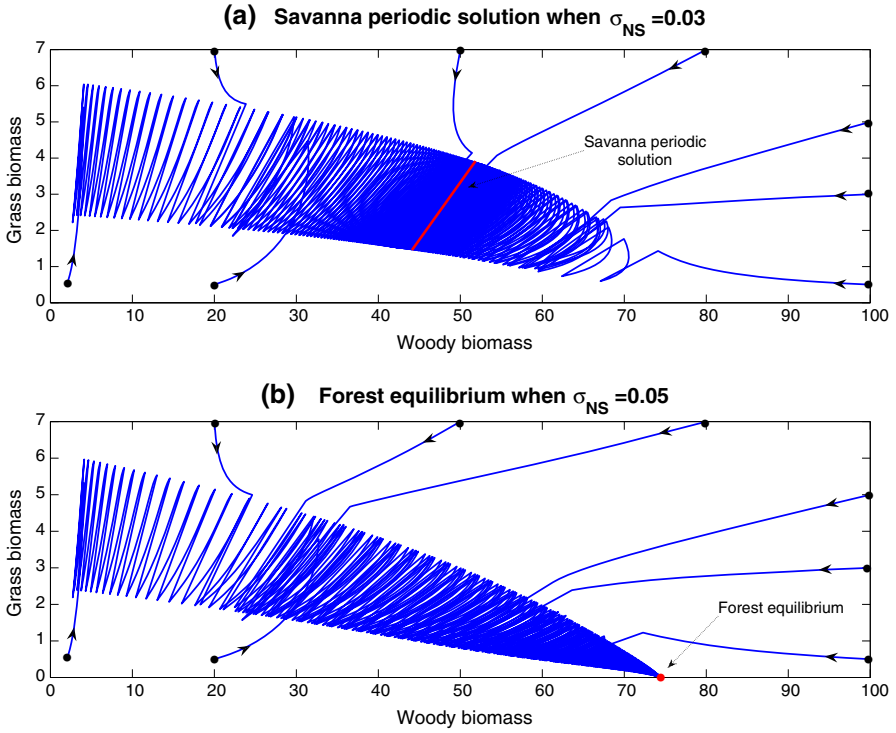

Fig. 7 Phase diagram of the IFAC illustrating a savanna to forest transition in Region 2. In **a** with $\tau = 2$, $K_T = 80$, $\sigma_G = 0.2$ and $\sigma_{NS} = 0.03$ the savanna periodic solution is stable while in **b** with $\tau = 2$, $K_T = 80$, $\sigma_G = 0.2$ and $\sigma_{NS} = 0.05$ the forest equilibrium (*red bullet*) is stable. Moreover, **a** illustrates case 1 of Table 1 with $\rho_{TG} = 0.8008$ and **b** illustrates case 4 of Table 1 with $\rho_T^G = 0.9472$ and the savanna solution being numerically unstable. The rest of the parameters are given in Table 7, p.27 (color figure online)

can also mention the fire-return time τ. In other words, the previous analysis reveals that in Region 2, in addition to stability of forest, stability of savanna and bistability of forest and savanna as in Region 1, one can observe stability of grassland and also multistabilty situations involving grassland solution with relatively low values of σ_G in comparison with Region 1.

We further provide a numerical simulation (Fig. 10, p. 33) that illustrates the richness of the outcomes of the impulsive modelling of fire events in comparison to the analogous time-continuous modelling (i.e. COFAC). From Tables 2 (p. 20) and 4 (p. 21), let us consider parameter values given in Table 8, p. 33. In Fig. 10, p. 33, the IFAC exhibits a bistability involving savanna and forest solutions while the COFAC exhibits the monostability of the savanna solution.

5.3 Results for Region 3

Region 3 corresponds to humid tropical areas where rainfall availability favors biomass production of both woody and grasses components. Forest is expected to be present

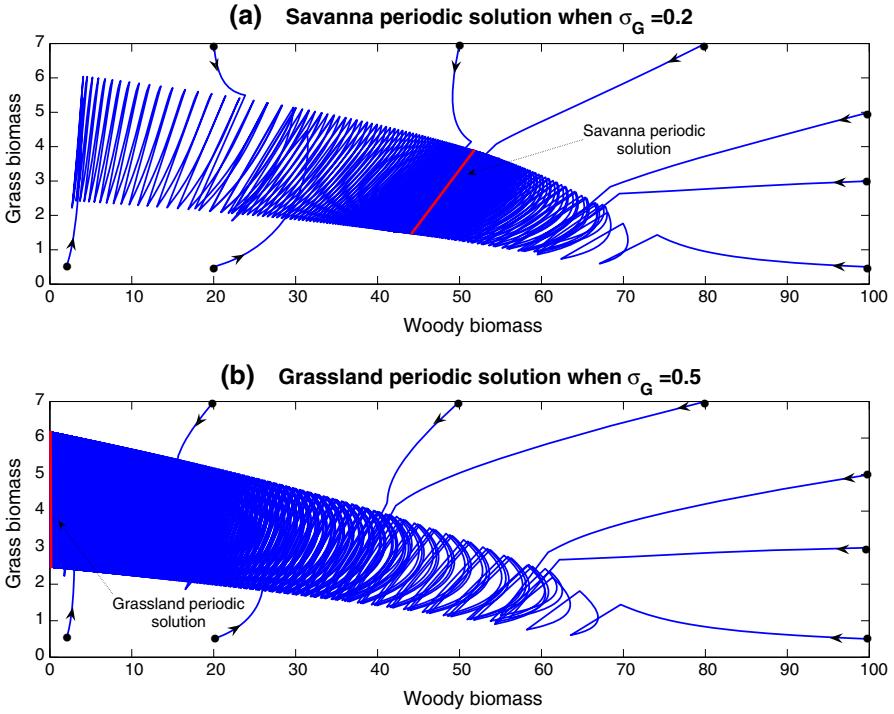

Fig. 8 Phase diagram of the IFAC illustrating a savanna to grassland transition in Region 2. In **a** with $\tau = 2$, $K_T = 80$, $\sigma_G = 0.2$ and $\sigma_{NS} = 0.03$ the savanna periodic solution is stable while in **b** with $\tau = 2$, $K_T = 80$, $\sigma_G = 0.5$ and $\sigma_{NS} = 0.03$ the grassland periodic solution is stable. Moreover, **a** illustrates case 1 of Table 1 with $\rho_{TG} = 0.8008$ and **b** illustrates case 2 of Table 1 with $\rho_T = 0.9931$ and the savanna solution being numerically unstable. The rest of the parameters are given in Table 7, p.27

in most of the landscapes. The grass-fire feedback possibly leads to stability of either savanna or forest in Region 3 depending on fire-return time. But grass particularly abundant in these wet areas, becomes an extremely good fuel in the dry season, which promotes fire occurrence and increases fire intensity and impact (Higgins et al. 2008; Baudena et al. 2014; Jeffery et al. 2014). When the fire-return time is large, the trees have the time to grow above the flame zone and to reach canopy closure and then suppress grasses. Therefore, relatively large return time favor forest states in Region 3 (Bond et al. 2005; Bond 2008; Staver and Levin 2012; Baudena et al. 2014; Jeffery et al. 2014). Conversely, if the fire-return time is small then trees don't have the time to reach canopy closure and therefore let grasses which regrow quickly in the open space after fires keep stands of high ignitable biomass that allow for stable savanna or grassland states. We illustrate hereafter that all these features are also predicted by the IFAC.

Consider

In this section, we will refer to a particular area, namely the Lamto region in Ivory Coast (see Menaut and César 1979; Mordelet and Menaut 1995) thanks to Abbadie et al. (2006) p. 156 data on the grass biomass. Abbadie et al. (2006) compared grass

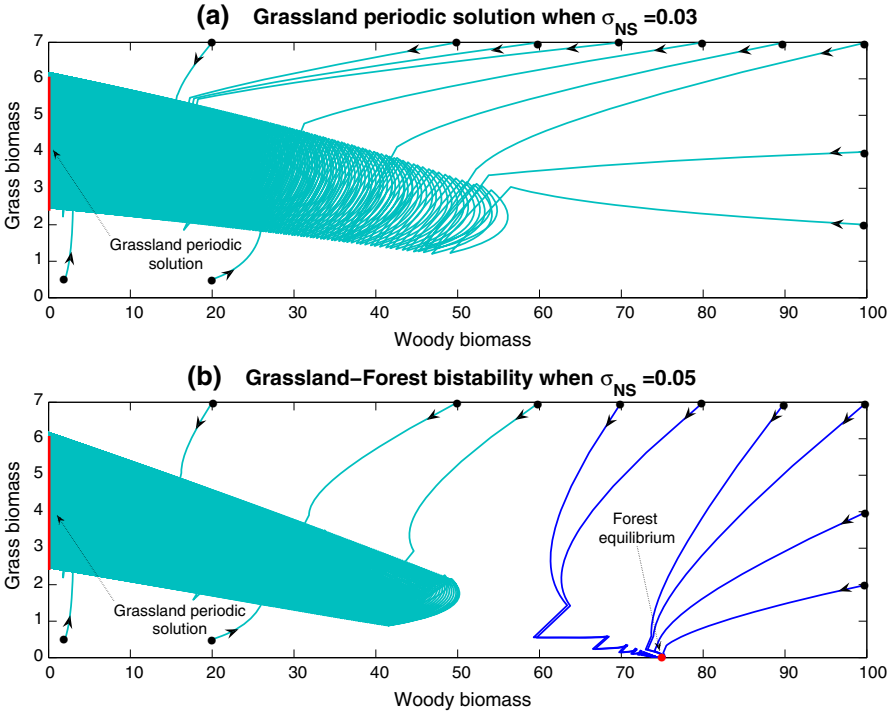

Fig. 9 Phase diagram of the IFAC illustrating a grassland to a grassland-forest bistability transition in Region 2. In **a** with $\tau = 2$, $K_T = 80$, $\sigma_G = 0.5$ and $\sigma_{NS} = 0.03$ the grassland periodic solution is stable while in **b** with $\tau = 2$, $K_T = 80$, $\sigma_G = 0.5$ and $\sigma_{NS} = 0.05$ the grassland periodic solution and the forest equilibrium are simultaneously stable. Moreover, **a** illustrates case 2 of Table 1 with $\rho_T = 0.9931$ and **b** illustrates case 5 of Table 1 with $\rho_T = 0.9931$, $\rho_T^G = 0.9472$ and the savanna solution being numerically unstable. The rest of the parameters are given in Table 7, p.27

production under the canopy and outside in Lamto. Reinterpreting their results we have derived that $\sigma_{NS} \in [0.0609, 0.0913]$.

Using parameter values in Table 9, p. 33, one has: $\mathcal{R}_T^0 = 35$, $\mathcal{R}_G^0 = 21$. We also derived the following Figs. 11 and 12 (p. 34).

Since for parameter values in Table 9 and according to our estimation of σ_{NS} one has

- $\mathcal{R}_T^G < 1$, $\rho_T^G < 1$,
- $\mathcal{R}_G^0 > 1$ then,

$$\rho_G^0 > 1 \Longleftrightarrow \tau > 0.2291.$$

Values of τ are not expected to be under 0.5 (i.e. 2 fires per year), a minimum which corresponds to sub-equatorial climates with two dry seasons (Jeffery et al. 2014). We therefore consider that this condition is always fulfilled.

Therefore, one can deduce that Fig. 11, p. 34, illustrates either case 8, 9 or case 10 of Table 1, p. 17. The previous analysis highlighted the importance of the grass biomass vs. sensitive tree biomass competition parameter, σ_G, the non-sensitive tree biomass vs.

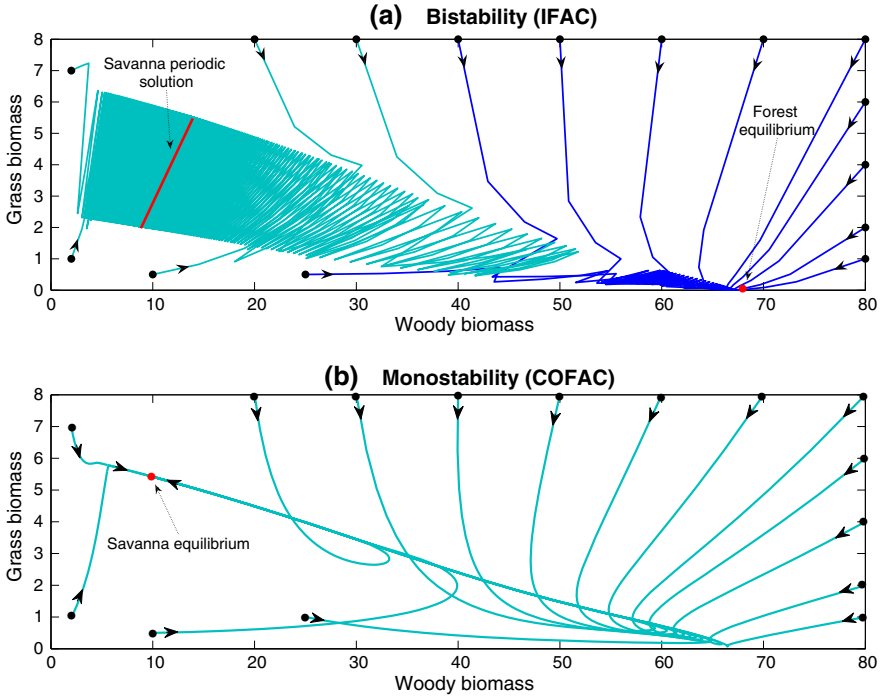

Fig. 10 Comparison of the **a** pulse (IFAC) vs. **b** continuous (COFAC) models in reference to Region 2. The impulsive fire model (IFAC) shows two solutions that are simultaneously stable: the savanna (as for the time-continuous model) and the forest (see **a**). In contrary, the time-continuous fire model (COFAC) presents a savanna equilibrium which is GAS (see **b**, *red bullet*). In the first case (**a**), depending of the initial conditions (*black bullets*) the system converges to a stable periodic savanna (*red line*) or to a stable forest equilibrium (*red bullet*). Moreover, **a** also illustrates case 4 of Table 1 (color figure online)

Table 8 Parameter values for Fig. 10

γ_S	γ_{NS}	γ_G	μ_{NS}	ω_S	η_S	η_G	μ_S
0.6	2	2.1	0.3	0.05	0.5	0.7	0.1
K_T	K_G	μ_G	$G0$	τ	σ_{NS}	σ_G	
80	9	0.3	2	2	0.13	0.08	
$\mathcal{R}_G^0$	$\mathcal{R}_T^0$	$\mathcal{R}_T^G$	ρ_G^0	ρ_T^G	$\mathcal{R}_G^T$	ρ_T	ρ_{TG}
7	6.2222	1.3575	10.9795	0.9068	1.6644	1.0561	0.7998

Table 9 Array of parameter' values for Region 3

γ_S	γ_{NS}	γ_G	μ_{NS}	ω_S	η_S	η_G	μ_S	μ_G
2	3	4.2	0.06	0.1	0.5	0.6	0.1	0.2

$K_T = 115$, $K_G = 15$, $G0 = 2$

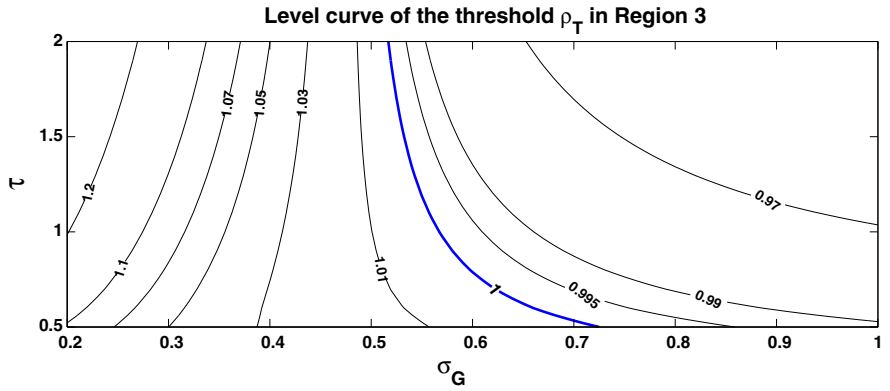

Fig. 11 Level curves of the threshold ρ_T illustrating that system (1, 2) is liable to move from a savanna/forest state to a grassland state or to a multistability involving the grassland solution in relation to τ and σ_G variations. Recall that the grassland solution is stable (resp. unstable) whenever ρ_T is lower (resp. greater) than unity

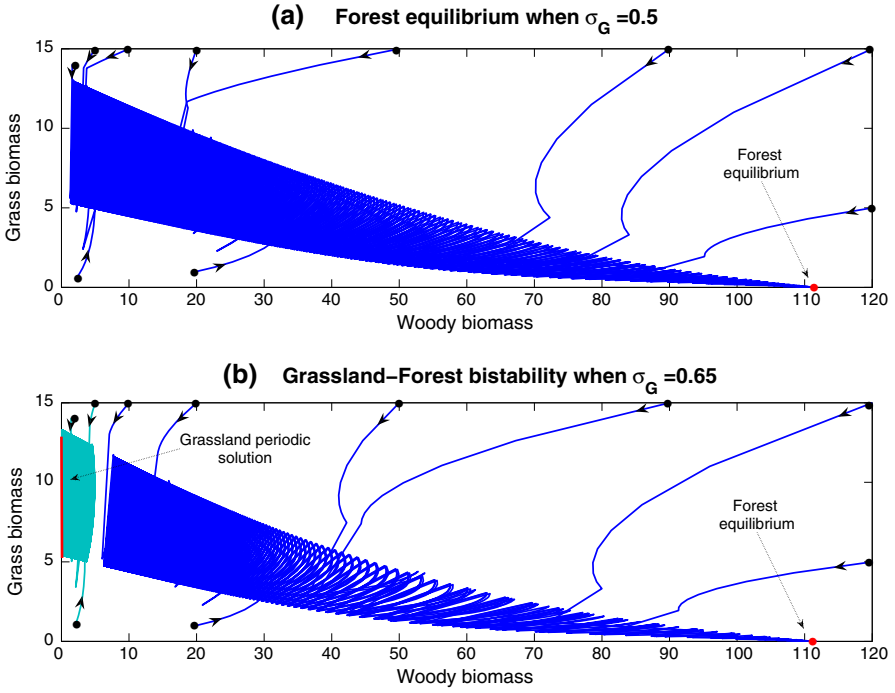

Fig. 12 Phase diagram of the IFAC illustrating a forest to a grassland-forest bistability transition in Region 3. In **a** with $\tau = 1, \sigma_G = 0.5$ and $\sigma_{NS} = 0.08$ the forest equilibrium is stable while in **b** with $\tau = 1, \sigma_G = 0.65$ and $\sigma_{NS} = 0.08$ the grassland periodic solution and the forest equilibrium are simultaneously stable. Moreover, **a** illustrates case 8 of Table 1 with $\rho_T^G = 0.0819$ and the savanna solution being numerically unstable. **b** illustrates case 10 of Table 1 with $\rho_T = 0.9909$, $\rho_T^G = 0.0819$ and the savanna solution being numerically unstable. The rest of the parameters are given in Table 9, p. 33

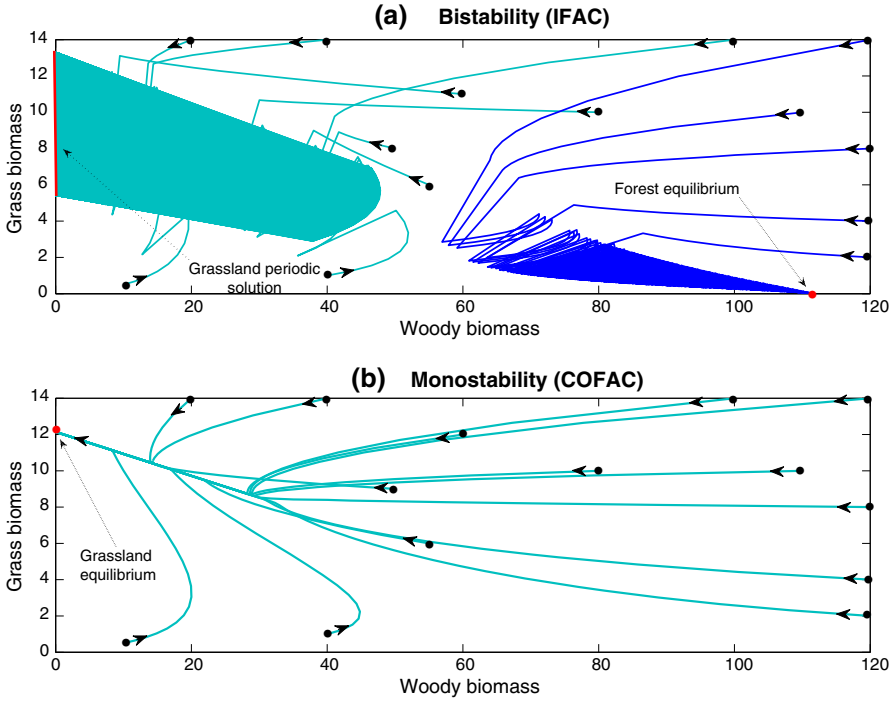

Fig. 13 Comparison of the **a** pulse (IFAC) vs. **b** continuous (COFAC) models in reference to Region 3. The impulsive fire model (IFAC) shows two solutions that are simultaneously stable: the grassland (as for the time-continuous model) and the forest (see **a**). In contrary, the time-continuous fire model (COFAC) presents a grassland equilibrium which is GAS (see **b**, *red bullet*). For the IFAC (**a**), depending of the initial conditions (*black bullets*) the system converges to a stable periodic grassland (vertical red line) or to a stable forest equilibrium (*red bullet*). $\tau = 1$, $\sigma_{NS} = 0.048$ and $\sigma_G = 0.7$. The rest of the parameters are given in Table 9, p. 33. Furthermore, **a** illustrates case 6 of Table 1 (color figure online)

grass biomass competition parameter, σ_{NS}, and the fire-return time, τ, in controlling the outcomes of the IFAC. Fig. 11, p. 34, further shows that for low values of σ_G, say less than 0.6, τ seems to have very limited influence. It has more influence for large values for which increases in τ make ρ_T decreases under 1 and therefore destabilizes the grassland solution.

In summary, in Region 3, we observed that the fire-return time along with σ_G and σ_{NS} strongly influence the outcome of the IFAC. Indeed, depending on these parameter variations and values, the IFAC can converge either to a grassland state, to a savanna state, to a forest state or to a multistability involving forest and either grassland or savanna while environmental conditions in this region would systematically allow forests in the absence of fire (Bond et al. 2005; Bond 2008; Staver and Levin 2012; Baudena et al. 2014; Jeffery et al. 2014). Therefore to favor a forest state in Region 3, one could implement policies in order to have relatively large fire-return time (says a fire frequency, f, lower than one fire per year: $f < 1$) and vice versa if tracts of savanna are to be kept against forest encroachment as habitats of large grazing mammals.

In order to illustrate the richness of the outcomes of the impulsive modelling of fire events in comparison to the time-continuous modelling, let us consider parameter

values given in Table 9, p. 33. We obtain Fig. 13, p. 35, which is also congruent with Favier et al. (2012) results. Indeed, around the latitude of 4° north along a general transect of the central tropical Africa (south of Cameroon—north-west of the Democratic Republic of Congo—south-west of the Central African Republic) which corresponds to Region 3, Favier et al. (2012) highlighted a very large range of woody cover variations (from very low values approaching grassland to nearly 80 % cover, i.e. forest) which strongly suggest grassland/forest bistability.

6 Conclusion-discussion

In this work, we presented and analyzed a new kind of mathematical model for tree–grass interactions in savanna ecosystems either fire prone or not. It is a direct extension of a continuous-time model, called the continuous fire model of asymmetric tree–grass competition (COFAC), studied in Yatat et al. (2014). All the founding ecological assumptions of COFAC have been kept, the crucial difference being in the modelling of fire occurrences. The model presented here, that we call the impulsive fire model of asymmetric tree–grass competition (IFAC), is based on a framework featuring impulsive differential equations and thereby aims to acknowledge the discrete nature of fire events while keeping the continuous framework for vegetation growth and direct interactions between plant forms. Since most of available data on fire occurrences are given in terms of fire-return time or fire period (Scholes and Archer 1997; Van Langevelde et al. 2003; Van Wilgen et al. 2004; Abbadie et al. 2006; Sankaran et al. 2008; Accatino et al. 2010; Calabrese et al. 2010; Staver and Bond 2014), for simplicity, here we chose to model periodic fires. The analytical study of the IFAC reveals that the model has the potential to predict a desert equilibrium, a forest equilibrium as well as a grassland periodic solution and a savanna periodic solution, that is all the main physiognomies encountered along the rainfall gradients observable in the inter-tropical zones. This is not achieved by all the existing models, even the ones that distinguish three vegetation components (e.g. Staver et al. 2011). The analytical study also reveals seven ecological thresholds ($\mathcal{R}_T^0$, $\mathcal{R}_G^0$, ρ_G^0, $\mathcal{R}_G^T$, $\mathcal{R}_T^G$, ρ_T^G, ρ_T) which define in parameter space regions of monostability and bistability also found with the models of Accatino et al. (2010), De Michele et al. (2011), Yatat et al. (2014), Tchuinté et al. (2014). Nevertheless, contrary to Accatino et al. (2010) and De Michele et al. (2011), the aforementioned thresholds also define in parameter space regions of grassland-savanna bistability. Finally, they also define regions of tristability as in Yatat et al. (2014) with respect to the forest equilibrium and periodic solutions (grassland and savanna). This is a novel and far-reaching result since a frequent and founded criticism against differential equation models is that they only predict abrupt shifts between highly contrasted physiognomies which have not yet been documented in the real-world (Higgins et al. 2000; Beckage et al. 2011; Accatino and De Michele 2013). Therefore, Accatino and De Michele (2013) (see also Higgins et al. 2000; Beckage et al. 2011) advocated stochastic models in lieu of continuous time formulation of fire impact on vegetation. The possible tristability provides a sufficiently rich set of outcomes to account for transitions implying intermediate levels of biomass (e.g. around the savanna equilibrium) either stable or not, while having the potential to also render

fire-maintained bistability between contrasting physiognomies, where it is suspected to exist (e.g. in equatorial conditions). Moreover, shifting the ω function from a type-2 to a type-3 sigmoid can determine an additional savanna equilibrium as evidenced in Yatat et al. (2014). The specificity of IFAC is to also present periodic behaviors which depict fluctuations in woody and/or grassy biomass in relation to fire occurrences. This cannot be yielded by fully continuous time models. The present approach however demonstrates that a more realistic modeling of fire can be introduced within the framework of continuous time models while keeping the potential for analytical exploration of the stability of the main outcomes of the model. Indeed stability of the desert, the forest and the grassland solutions are analytically characterized while we needed numerical simulations just to discuss the stability of the savanna solution. Something which is not always granted with the fully stochastic models (Higgins et al. 2000; Beckage et al. 2011; Accatino and De Michele 2013).

As in Yatat et al. (2014), we found that the competition parameters σ_G which expresses the asymmetric competition exerted by grasses on small, fire-sensitive trees (shading and soil resource preemption) and σ_{NS} that expresses the asymmetric competition of non-sensitive trees on grasses (shading and soil resource preemption) are bifurcation parameters of the IFAC along with fire frequency. The analytical study of the IFAC also reveals three particular values $\tau^\star$, $\sigma_{NS}^\star$ and $\sigma_G^\star$ (see relation (89), p. 55) that delimit regions of stability/instability of forest and grassland solutions in relation to τ, σ_{NS} and σ_G respectively (see relations (13), p. 11 and (17), p. 12). Moreover, considering three ecological biomass production zones indexed by fires frequency and by carrying capacities of both trees and grasses biomasses, allows us to point out several scenarios for IFAC convergence that depend notably on σ_G, σ_{NS} and τ values. Distinguishing three main ecological regions allowed us to verify in which contexts the possible bifurcation parameters are actually influential or not. This analysis highlighted the pervasiveness of σ_{NS} (i.e. the effect of grown-up trees on grasses) in all the three regions whatever the type of fire regime induced by the climate. It also emphasized the influence of σ_G (i.e. depressive effect of grasses on small trees) in the two regions (2 and 3) with sufficient rainfall to allow medium to high grass biomass production and regular fire occurences. In these two regions, and especially in Region 3, the fire-return time (τ) appeared also influential. As already mentioned by Yatat et al. (2014), and verified here for the IFAC, the competition parameters σ_G and σ_{NS} which embody direct tree–grass interactions deserve an increased interest and should be the focus of adhoc observations and experiments as to better assess their ranges of variation in the different ecological regions. To authors' knowledge, it is the first time that a mathematical model of savanna dynamics highlights a direct and crucial role for parameters analogous to σ_G and σ_{NS}. It suggests that not only fires but also direct interactions between plant types are contributors to the dynamical properties of these systems. (But see Tchuinté et al. 2014, regarding the homologue of σ_{NS}.)

Although the IFAC presented in this work and the COFAC presented in Yatat et al. (2014) qualitatively display strong similarities, the IFAC is richer in terms of possible outcomes (see Fig. 10, p. 33, Fig. 13, p. 35, Remark 7, p. 13). Indeed modelling fire events as pulse phenomena leads to a relaxation of stability conditions of both forest and grassland solutions (see Remark 7, p. 13) which increases parameter ranges for which bistability situations involving forest, grassland and savanna can occur (see Figs.

10, 13). This particular property of the IFAC may in the future help explain a variety of empirical evidences regarding the dynamics of savanna-like ecosystems (either fire-prone or not). The dynamical nature of these ecosystems has inspired a wealth of modelling studies over the last decade. But broad scale monitoring is still in its infancy in spite of recent and impressive breakthroughs (Hirota et al. 2011; Favier et al. 2012; Mermoz et al. 2015). Diversifying remote sensing capabilities indeed open avenues to detect and characterize non-trivial and varied dynamical phenomena across the savanna biome. Models are important tools to bridge the scale gap between local field data (e.g. refined local assessment of σ_{NS}, σ_G, etc.) and remote-sensing broad scale information on physiognomies. Conversely, the availability of new sources of data will submit the models to increasingly demanding tests about their relevance or generality. Thanks to its innovative structure integrating time-continuous and impulsive equations, the IFAC which displays periodic outcomes, varied mono, bistability and tristability schemes, and bifurcations according to well-identified parameters, is able to account for many dynamical scenarios observed in savanna-like ecosystems from the fringes of the desert to the boundary of the wet forest.

A possible extension of the current study could consist in explicitly taking into account spatial mechanisms of tree–grass interactions in a mathematical model. Two major spatial mechanisms in tree–grass interactions are seedlings establishment and tree–grass competition and/or facilitation (Pueyo et al. 2010). While facilitation is a local process, competition for limiting resources (mainly water in arid and semi-arid environments) can occur at a larger spatial scale (Gilad et al. 2007; Barbier et al. 2008; Lefever et al. 2009; Pueyo et al. 2010). Most of available mathematical models that take into account spatial mechanisms are designed for regions where water is the most limiting factor and fires are unfrequent (Gilad et al. 2007; Pueyo et al. 2008, 2010; Lefever et al. 2009; Baudena and Rietkerk 2013). Therefore, in a forthcoming study we intend to present a mathematical model designed for fire-prone savannas that explicitly acknowledges spatial mechanisms of tree–grass interactions together with discrete fire events.

Acknowledgements Thanks to the reviewers for insightful comments that helped us to improve the paper. The first author is grateful to the French government and the SCAC service of the French Embassy in Yaoundé (Cameroon) for their support (SCAC fund) during the preparation of this manuscript.

7 Appendix: Proof of Lemma 1

Let $([t_0 = 0, \beta), X(t) = (T_S, T_{NS}, G)(t))$ be a solution of the system (1–3). Since at any pulse moment, one has

$$\begin{cases} T_S(t_k^+) &= (1-\eta_S w(G(t_k)))T_S(t_k) \leq T_S(t_k), \\ T_{NS}(t_k^+) &= T_{NS}(t_k) \qquad\qquad\quad \leq T_{NS}(t_k), \quad t_{k+1} = t_k + \tau,\ k = 1, 2, 3, \ldots \\ G(t_k^+) &= (1-\eta_G)G(t_k) \qquad\quad \leq G(t_k), \end{cases}$$

thus, in order to prove that solutions of system (1, 2) remain positive for positive initial data and that there are bounded, it suffices to establish these results for $t \in [0, \beta)$, $t \neq t_k$.

(i) Let suppose that the solution X starts in the positive orthant $\mathbb{R}^3_+$. To become negative, X must cross one of three borders of $\mathbb{R}^3_+$. In other words, X must cross one of the sets $\{T_S = 0\}$, $\{T_{NS} = 0\}$, $\{G = 0\}$. So, to prove that system (1, 2) is positively invariant, we only need to show that at any borders of $\mathbb{R}^3_+$, either the resulting vector field stays on the border or is pointing inside $\mathbb{R}^3_+$.

Case 1: $\{G = 0\}$. At this border and following the third equation of system (1), one has $\dfrac{dG}{dt} = 0$. Consequently, the solution X can not cross $\mathbb{R}^3_+$ through the border $\{G = 0\}$.
Case 2: $\{T_{NS} = 0\}$. Following the second equation of system (1), one has $\dfrac{dT_{NS}}{dt} = \omega_S T_S \geq 0$. Therefore, the solution X can not cross $\mathbb{R}^3_+$ through the border $\{T_{NS} = 0\}$.
Case 3: $\{T_S = 0\}$. From the first equation of system (1), one has

$$\frac{dT_S}{dt} = \gamma_{NS} T_{NS} \left(1 - \frac{T_{NS}}{K_T}\right). \tag{37}$$

To conclude, we need to prove that on the border $\{T_S = 0\}$, one has $T_{NS} \leq K_T$. From the second equation of system (1) one has $(T_{NS})'(t) = -\mu_{NS} T_{NS} \leq 0$ on the border $\{T_S = 0\}$. Therefore, for all $0 \leq t < \beta$, $T_{NS}(t) \leq T_{NS}(0) \leq K_T$. Consequently, part 1 of Lemma 1 holds.

(ii) From system (1) we deduce that T_S, T_{NS} and G are such that

$$\begin{cases} T_S' + T_{NS}' \leq (\gamma_S T_S + \gamma_{NS} T_{NS}) \left(1 - \dfrac{T_S + T_{NS}}{K_T}\right) - \mu_S T_S - \mu_{NS} T_{NS}, \\ G' \leq \gamma_G \left(1 - \dfrac{G}{K_G}\right) G. \end{cases} \tag{38}$$

Let us set $T = T_S + T_{NS}$. Concerning γ_S and γ_{NS}, one has three possibilities: (a) $\gamma_S = \gamma_{NS}$; (b) $\gamma_S < \gamma_{NS}$ and (c) $\gamma_S > \gamma_{NS}$.

In case (a), from system (38) we deduce

$$\begin{cases} T' \leq \gamma_S \left(1 - \dfrac{T}{K_T}\right) T, \\ G' \leq \gamma_G \left(1 - \dfrac{G}{K_G}\right) G. \end{cases} \tag{39}$$

Using a comparison argument (see also Tchuinté et al. 2014) we deduce that $T \leq K_T$ and $G \leq K_G$. Thus according to i), Ω is an invariant bounded region for system (1–3).

In case (b), let us set $\varepsilon = \gamma_{NS} - \gamma_S > 0$. From the first inequality of system (38) we deduce $T' \leq \gamma_S T \left(1 - \dfrac{T}{K_T}\right) + (\varepsilon - \mu_{NS}) T_{NS}$. Thus, if $\varepsilon \leq \mu_{NS}$ then we are in

case (a) and the conclusion is valid. Otherwise, from system (38) we have

$$\begin{cases} T' \leq (\gamma_{NS} - \mu_{NS}) \left(1 - \dfrac{\gamma_S T}{(\gamma_{NS} - \mu_{NS}) K_T}\right) T, \\ G' \leq \gamma_G \left(1 - \dfrac{G}{K_G}\right) G. \end{cases} \tag{40}$$

Thus, following case (a), the conclusion is valid. Finally case (c) can be done similarly as case (b) with γ_S instead of γ_{NS} and μ_S instead of μ_{NS}.

8 Appendix: Proof of Lemma 4

Defining

$$\begin{aligned} T_S(t) &= x(t), \\ T_{NS}(t) &= y(t), \\ G(t) &= G^*(t) + z(t), \end{aligned} \tag{41}$$

where $x(t)$, $y(t)$ and $z(t)$ are small perturbations. Every solution of the linearized equations can be written as

$$\begin{pmatrix} x(t) \\ y(t) \\ z(t) \end{pmatrix} = \Phi(t) \begin{pmatrix} x(0) \\ y(0) \\ z(0) \end{pmatrix}. \tag{42}$$

Here Φ is a fundamental matrix and satisfies,

$$\begin{aligned} \frac{d\Phi(t)}{dt} &= DF(0, 0, G^*(t))\Phi(t) \\ &= \begin{pmatrix} \gamma_S - (\mu_S + \omega_S + \sigma_G G^*(t)) & \gamma_{NS} & 0 \\ \omega_S & -\mu_{NS} & 0 \\ 0 & -\sigma_{NS} G^*(t) & \gamma_G - 2\dfrac{\gamma_G}{K_G} G^*(t) - \mu_G \end{pmatrix} \Phi(t) \end{aligned} \tag{43}$$

and $\Phi(0) = Id_{\mathbb{R}^3}$. Moreover the resetting impulsive condition of system (1, 2) becomes,

$$\begin{pmatrix} x(n\tau^+) \\ y(n\tau^+) \\ z(n\tau^+) \end{pmatrix} = \begin{pmatrix} 1 - \eta_S w(G^*(\tau)) & 0 & 0 \\ 0 & 1 & 0 \\ 0 & 0 & 1 - \eta_G \end{pmatrix} \begin{pmatrix} x(n\tau) \\ y(n\tau) \\ z(n\tau) \end{pmatrix}. \tag{44}$$

A monodromy matrix $\mathbf{M}$ of system (1, 2), is:

$$\mathbf{M} = \begin{pmatrix} 1 - \eta_S w(G^*(\tau)) & 0 & 0 \\ 0 & 1 & 0 \\ 0 & 0 & 1 - \eta_G \end{pmatrix} \Phi(\tau), \tag{45}$$

with

$$\Phi(t) \;=\; \exp\left(\int_0^t DF(0,0,G^*(s))ds\right). \tag{46}$$

Moreover using Lemma 3, a direct computations leads

$$\int_0^\tau DF(0,0,G^*(s))ds = \begin{pmatrix} DF^{(1)} & DF^{(2)} & 0 \\ DF^{(3)} & DF^{(4)} & 0 \\ 0 & DF^{(5)} & DF^{(6)} \end{pmatrix},$$

where

$$\begin{aligned} DF^{(1)} &= (\gamma_S - (\mu_S + \omega_S))\tau - \sigma_G \int_0^\tau G^*(t)dt, \\ DF^{(2)} &= \gamma_{NS}\tau, \\ DF^{(3)} &= \omega_S\tau, \\ DF^{(4)} &= -\mu_{NS}\tau, \\ DF^{(5)} &= -\sigma_{NS} \int_0^\tau G^*(t)dt, \\ DF^{(6)} &= -\mu_G(\mathcal{R}_G^0 - 1)\tau - 2\ln(1-\eta_G). \end{aligned} \tag{47}$$

Consider the sub-matrix $\mathbf{B}$ defined as follow:

$$\mathbf{B} = \begin{pmatrix} DF^{(1)} & DF^{(2)} \\ DF^{(3)} & DF^{(4)} \end{pmatrix}. \tag{48}$$

Recall that eigenvalues of the matrix $\mathbf{B}$ are roots of the quadratic equation

$$\lambda^2 - trace(\mathbf{B})\lambda + \det(\mathbf{B}) = 0$$

and to characterize real part of eigenvalues of matrix $\mathbf{B}$, following Routh–Hurwitz criterium (see Sect. 1.3.5 P. 72 of Augier et al. 2010), we need only to study the sign of $trace(\mathbf{B})$ and $\det(\mathbf{B})$. Let

$$\mathcal{A} = tr(\mathbf{B}) = \gamma_S\tau\left(1 - \frac{1}{\mathcal{R}}\right), \tag{49}$$

where

$$\mathcal{R} = \frac{\gamma_S}{\mu_S + \omega_S + \mu_{NS} + \sigma_G G_{int}} > 0.$$

Thus, if $\mathcal{R} < 1$ then $\mathcal{A} < 0$.

Moreover, let

$$\mathcal{B} = \det(\mathbf{B}) = \tau\mu_{NS}\left((\mu_S + \omega_S)\tau + \sigma_G G_{int}\right)\left(1 - \mathcal{R}_G^T\right), \tag{50}$$

where

$$\mathcal{R}_G^T = \frac{\gamma_S \mu_{NS} + \omega_S \gamma_{NS}}{\mu_{NS}(\mu_S + \omega_S) + \sigma_G \mu_{NS} G_{int}} > 0.$$

Thus, if $\mathcal{R}_G^T < 1$ then $\mathcal{B} > 0$.

Moreover, one also has $\mathcal{R} < \mathcal{R}_G^T$.

Therefore, if $\mathcal{R}_G^T < 1$ then $s(\mathbf{B}) < 0$, where s denotes the stability modulus (i.e. the maximum of the real part of eigenvalues).

From expressions (45) and (46) we deduce that eigenvalues ξ_1, ξ_2 and ξ_3 of the monodromy matrix $\mathbf{M}$ are

$$\begin{aligned} \xi_1 &= (1 - \eta_S w(G^*(\tau)))e^{\lambda_1}, \\ \xi_2 &= e^{\lambda_2}, \\ \xi_3 &= \frac{e^{-\mu_G(\mathcal{R}_G^0 - 1)\tau}}{1 - \eta_G}, \end{aligned} \tag{51}$$

where $\lambda_1, \lambda_2 \in sp(\mathbf{B})$. Since $0 < 1 - \eta_S w(G^*(\tau)) \leq 1$, if $\mathcal{R}_G^T < 1$, then $0 \leq \xi_1 < 1$ and $0 < \xi_2 < 1$.

Moreover, since $\rho_G^0 > 1$ then $\xi_3 < 1$. Indeed,

$$\xi_3 < 1 \Leftrightarrow e^{-\mu_G(\mathcal{R}_G^0 - 1)\tau} < 1 - \eta_G \Leftrightarrow 1 < (1 - \eta_G)e^{\mu_G(\mathcal{R}_G^0 - 1)\tau} \Leftrightarrow \rho_G^0 > 1.$$

Finally we deduce that the grassland periodic solution $E_G = (0; 0; G^*(t))$ is locally asymptotically stable if $\mathcal{R}_G^T < 1$ or ($\mathcal{R}_G^T > 1$ and $\rho_T < 1$), is locally stable if ($\mathcal{R}_G^T > 1$ and $\rho_T = 1$) and is unstable if ($\mathcal{R}_G^T > 1$ and $\rho_T > 1$). This ends the proof.

9 Appendix: Proof of Theorem 1

⋆ Case 1: $\mu_G > 0$. Solution G of system (1, 2) satisfy

$$\begin{aligned} G'(t) &\leq \gamma_G \left(1 - \frac{1}{\mathcal{R}_G^0}\right) G(t) \\ G(t_k^+) &= (1 - \eta_G) G(t_k). \end{aligned} \tag{52}$$

From Lemma 1.3 page 15 in Bainov and Simeonov (1995) we deduce that

$$G(t) \leq G(0) \left(\prod_{0 \leq t_k < t} (1 - \eta_G) \right) \exp\left(\gamma_G \left(1 - \frac{1}{\mathcal{R}_G^0}\right) t \right).$$

Thus, for $\mathcal{R}_G^0 < 1$ we have $\lim_{t\to+\infty} G(t) = 0$ and solutions T_S and T_{NS} of system (1, 2) satisfy

$$\begin{cases} T_S' &= (\gamma_S T_S + \gamma_{NS} T_{NS})\left(1 - \dfrac{T_S + T_{NS}}{K_T}\right) - T_S(\mu_S + \omega_S), \\ T_{NS}' &= \omega_S T_S - \mu_{NS} T_{NS}. \end{cases} \tag{53}$$

System (53) does not admit periodic solution (see Appendix B in Yatat et al. (2014)), thus using the jacobian matrix of system (53) we deduce that

- if $\mathcal{R}_T^0 < 1$ then, $(T_S, T_{NS}) \to (0, 0)$,
- if $\mathcal{R}_T^0 > 1$ then, $(T_S, T_{NS}) \to (\bar{T}_S, \bar{T}_{NS})$, where $(\bar{T}_S, \bar{T}_{NS})$ are given in (15).

At the end, we deduce that if $\mathcal{R}_T^0 < 1$ and $\mathcal{R}_G^0 < 1$ then, the desert equilibrium E_0 is GAS i.e., point 1 of Theorem 1 holds. The forest equilibrium E_T is GAS whenever $\mathcal{R}_T^0 > 1$ and $\mathcal{R}_G^0 < 1$ i.e., point 2 of Theorem 1 holds. Now suppose that $\mathcal{R}_T^0 < 1$ and $\mathcal{R}_G^0 > 1$. Solutions T_S and T_{NS} of system (1, 2) satisfy

$$\begin{cases} \dfrac{dT_S}{dt} &\le (\gamma_S T_S + \gamma_{NS} T_{NS})\left(1 - \dfrac{T_S + T_{NS}}{K_T}\right) - T_S(\mu_S + \omega_S), \\ \dfrac{dT_{NS}}{dt} &\le \omega_S T_S - \mu_{NS} T_{NS}, \qquad t \ne t_k \end{cases} \tag{54}$$

$$\begin{cases} T_S(t_k^+) &\le T_S(t_k), \\ T_{NS}(t_k^+) &\le T_{NS}(t_k), \ t = t_k \ t_{k+1} = t_k + \tau. \end{cases} \tag{55}$$

Let consider the upper system

$$\begin{cases} \dfrac{du}{dt} &= (\gamma_S u + \gamma_{NS} v)\left(1 - \dfrac{u + v}{K_T}\right) - u(\mu_S + \omega_S), \\ \dfrac{dv}{dt} &= \omega_S u - \mu_{NS} v, \end{cases} \tag{56}$$

Since $\mathcal{R}_T^0 < 1$, $(u(t), v(t)) \to (0, 0)$. Thus $(T_S(t), T_{NS}(t)) \to (0, 0)$. Furthermore, solution G of system (1, 2) admits as limiting system

$$\begin{cases} \dfrac{dG}{dt} &= \gamma_G\left(1 - \dfrac{G}{K_G}\right) G - \mu_G G \ t \ne t_k, \\ G(t_k^+) &= (1 - \eta_G) G(t_k) \qquad t = t_k. \end{cases} \tag{57}$$

System (57) admits at most two solutions: the trivial solution, 0, which always exists and the periodic solution $G^*(t)$ which is ecologically meaningful if $\rho_G^0 > 1$ where $G^*(t)$ is given by (8). Now we turn to check stability results of solutions of system (57) through small perturbations approach and Floquet's theory.

– Setting $G(t) = x(t)$ where x is a small perturbation and verifies $x(t) = \phi(t)x_0$, where ϕ verifies

$$\phi'(t) = \mu_G \left(\mathcal{R}_G^0 - 1\right) \phi(t)$$

and $\phi(0) = 1$. The resulting impulsive condition becomes

$$x(nT^+) = (1 - \eta_G)x(nT).$$

Following the Floquet's theory, the zero equilibrium is locally asymptotically stable if

$$\lambda_0 = (1 - \eta_G)e^{\mu_G(\mathcal{R}_G^0 - 1)\tau} < 1.$$

Since

$$\mathcal{R}_G^0 > 1, \lambda_0 < 1 \quad \text{if and only if } (1 - \eta_G)e^{\mu_G(\mathcal{R}_G^0 - 1)\tau} < 1, i.e. \rho_G^0 < 1.$$

Moreover, for $\rho_G^0 < 1$ the positive solution $G^*(t)$ is undefined then the desert equilibrium is globally asymptotically stable. Finally, we deduce that the desert solution $(0, 0, 0)$ is globally asymptotically stable whenever $\mathcal{R}_T^0 < 1$, $\mathcal{R}_G^0 > 1$ and $\rho_G^0 < 1$. Point 3 of Theorem 1 holds.

– Now, setting $G(t) = G^*(t) + x(t)$ where x is a small perturbation and verifies $x(t) = \phi(t)x_0$, where ϕ verifies

$$\phi'(t) = \left[\mu_G \left(\mathcal{R}_G^0 - 1\right) - \frac{2\gamma_G}{K_G} G^*(t)\right] \phi(t)$$

and $\phi(0) = 1$. The resulting impulsive condition becomes

$$x(nT^+) = (1 - \eta_G)x(nT).$$

According to the Floquet's theory, solution $G^*(t)$ is locally asymptotically stable if

$$\lambda_{G^*} = (1 - \eta_G) \exp\left\{\mu_G \left(\mathcal{R}_G^0 - 1\right) \tau - \frac{2\gamma_G}{K_G} \int_{n\tau}^{(n+1)\tau} G^*(t)dt\right\} < 1.$$

Following Lemma 3,

$$\int_{n\tau}^{(n+1)\tau} G^*(s)ds = \frac{K_G}{\gamma_G} \left\{\ln(1 - \eta_G) + \mu_G \left(\mathcal{R}_G^0 - 1\right) \tau\right\}. \tag{58}$$

Thus

$$\begin{aligned}\lambda_{G^*} &= (1-\eta_G)\exp\left\{-\mu_G\left(\mathcal{R}_G^0-1\right)\tau - 2\ln(1-\eta_G)\right\}\\ &= \exp\left\{-\mu_G(\mathcal{R}_G^0-1)\tau - \ln(1-\eta_G)\right\}.\end{aligned} \tag{59}$$

Since $\rho_G^0 > 1$, we have:

$$\begin{aligned}\rho_G^0 > 1 &\Leftrightarrow (1-\eta_G)\exp\{\mu_G(\mathcal{R}_G^0-1)\tau\} > 1\\ &\Leftrightarrow \ln(1-\eta_G) > -\mu_G(\mathcal{R}_G^0-1)\tau\\ &\Leftrightarrow -\mu_G(\mathcal{R}_G^0-1)\tau - \ln(1-\eta_G) < 0\end{aligned} \tag{60}$$

and we deduce

$$\lambda_{G^*} < 1.$$

Thus solution $G^*(t)$ of (57) is globally asymptotically stable because the zero solution, in this case, is unstable. Finally, we deduce that the grassland periodic solution $(0, 0, G^*(t))$ is globally asymptotically stable whenever $\mathcal{R}_T^0 < 1$, $\mathcal{R}_G^0 > 1$ and $\rho_G^0 > 1$. Point 4 of Theorem 1 holds.

⋆ Case 2: $\mu_G = 0$.

The proof of points (i) and (ii) of Theorem 1 is fairly the same as the proof of points 3 and 4. Indeed we first set, only in system (57), $\mu_G = 0$ and next, we substitute $\mu_G(\mathcal{R}_G^0 - 1)$ by γ_G in the rest of the proof.

Solutions G of system (1, 2) satisfy

$$\begin{cases}\dfrac{dG}{dt} \leq \gamma_G\left(1-\dfrac{G}{K_G}\right)G & t \neq t_k,\\ G(t_k^+) = (1-\eta_G)G(t_k) & t = t_k.\end{cases} \tag{61}$$

Since $\rho_G^0 = (1-\eta_G)\exp\{\gamma_G\tau\} < 1$, it follows that $G(t) \longrightarrow 0$. Therefore, solutions T_S and T_{NS} of (1, 2) satisfy system (53). Since $\mathcal{R}_T^0 < 1$, one has $(T_S,\ T_{NS}) \longrightarrow (\bar{T}_S,\ \bar{T}_{NS})$. Point (iii) of Theorem 1 holds.

10 Appendix: Proof of Theorem 2

Taking new variables $T_S(t) = e^{x(t)}$, $T_{NS}(t) = e^{y(t)}$, $G(t) = e^{z(t)}$ then system (1, 2) becomes,

$$\begin{cases} \dot{x}(t) &= -\omega_S - \mu_S - \sigma_G e^z + (\gamma_S + \gamma_{NS} e^y e^{-x}) \left(1 - \dfrac{e^x + e^y}{K_T}\right), \quad t \neq t_n. \\ \dot{y}(t) &= -\mu_{NS} + \omega_S e^x e^{-y}, \quad t_{n+1} = t_n + \tau, \\ \dot{z}(t) &= \gamma_G \left(1 - \dfrac{e^z}{K_G}\right) - \sigma_{NS} e^y - \mu_G, \\ x(t^+) &= x(t) + \ln(1 - \eta_S w(e^z)), \quad t = t_n. \\ y(t^+) &= y(t), \quad n = 0, 1, 2, \ldots, \\ z(t^+) &= z(t) + \ln(1 - \eta_G). \end{cases} \tag{62}$$

Let $X = C^1([0,\tau], \mathbb{R}^3)$, $Z = C^1([0,\tau], \mathbb{R}^3) \times C^1([0,\tau], \mathbb{R}^3)$ and for $u = (x, y, z) \in X$,

$$||u|| = \max_{t\in[0,\tau]} |x(t)| + \max_{t\in[0,\tau]} |y(t)| + \max_{t\in[0,\tau]} |z(t)|.$$

Then X, Z are Banach spaces when they are endowed with the above norm $||\cdot||$. Let,

$$L : Dom(L) \subset X \to Z, \begin{pmatrix} x \\ y \\ z \end{pmatrix} \to \left(\begin{pmatrix} \dot{x} \\ \dot{y} \\ \dot{z} \end{pmatrix}, \begin{pmatrix} \Delta x(t_n) \\ \Delta y(t_n) \\ \Delta z(t_n) \end{pmatrix} \right)$$

and

$$N \begin{pmatrix} x \\ y \\ z \end{pmatrix} = \left(N_1 \begin{pmatrix} x \\ y \\ z \end{pmatrix}, N_2 \begin{pmatrix} x \\ y \\ z \end{pmatrix} \right),$$

where

$$N_1 \begin{pmatrix} x \\ y \\ z \end{pmatrix} = \begin{pmatrix} -\omega_S - \mu_S - \sigma_G e^z + (\gamma_S + \gamma_{NS} e^y e^{-x}) \left(1 - \dfrac{e^x + e^y}{K_T}\right) \\ -\mu_{NS} + \omega_S e^x e^{-y} \\ \gamma_G \left(1 - \dfrac{e^z}{K_G}\right) - \sigma_{NS} e^y - \mu_G \end{pmatrix},$$

$$N_2 \begin{pmatrix} x \\ y \\ z \end{pmatrix} = \begin{pmatrix} \ln(1 - \eta_S w(e^{z(\tau)})) \\ 0 \\ \ln(1 - \eta_G) \end{pmatrix}.$$

A direct computation leads to

$$Ker L = \left\{ \begin{pmatrix} x \\ y \\ z \end{pmatrix} : \begin{pmatrix} x \\ y \\ z \end{pmatrix} = \begin{pmatrix} c_1 \\ c_2 \\ c_3 \end{pmatrix} \in \mathbb{R}^3, \ t \in [0,\tau] \right\}$$

and

$$ImL = \left\{ \left(\begin{pmatrix} l \\ m \\ n \end{pmatrix}, \begin{pmatrix} a \\ b \\ c \end{pmatrix} \right) \in Z : \begin{pmatrix} \int_0^\tau l(t)dt + a = 0 \\ \int_0^\tau m(t)dt + b = 0 \\ \int_0^\tau n(t)dt + c = 0 \end{pmatrix} \right\}.$$

Since ImL is closed in Z, L is a Fredholm mapping of index zero. Indeed,

$$\begin{aligned} Index(L) &= dim(KerL) - dim(CoKerL) \\ &= dim(KerL) - (dim(Z) - dim(ImL)) = 3 - (6 - 3) = 0. \end{aligned}$$

Thus following (Gaines and Mawhin 1977, P. 12), there exist two continuous projectors P and Q such that the sequel $X \xrightarrow{P} DomL \xrightarrow{L} Z \xrightarrow{Q} Z$ is exact i.e. $ImP = KerL$ and $KerQ = ImL = Im(I - Q)$. It suffices to choose

$$P \begin{pmatrix} x \\ y \\ z \end{pmatrix} = \begin{pmatrix} x(\tau) \\ y(\tau) \\ z(\tau) \end{pmatrix} \quad and \quad Q \left(\begin{pmatrix} l \\ m \\ n \end{pmatrix}, \begin{pmatrix} a \\ b \\ c \end{pmatrix} \right) = \left(\frac{1}{\tau} \begin{pmatrix} \int_0^\tau l(s)ds + a \\ \int_0^\tau m(s)ds + b \\ \int_0^\tau n(s)ds + c \end{pmatrix}, \begin{pmatrix} 0 \\ 0 \\ 0 \end{pmatrix} \right).$$

One can verify that $LP \begin{pmatrix} x \\ y \\ z \end{pmatrix} = 0_X$ and $QL \begin{pmatrix} x \\ y \\ z \end{pmatrix} = 0_Z$.

Furthermore, the generalized inverse $K_P : ImL \to KerP \cap Dom(L)$ of the map $L : KerP \cap Dom(L) \to ImL$ is given by

$$K_P \left(\begin{pmatrix} l \\ m \\ n \end{pmatrix}, \begin{pmatrix} a \\ b \\ c \end{pmatrix} \right) = \begin{pmatrix} \int_0^t l(s)ds + a \\ \int_0^t m(s)ds + b \\ \int_0^\tau n(s)ds + c \end{pmatrix}.$$

Indeed, let $u = (u_1, u_2, u_3)^T \in KerP \cap Dom(L)$, $(g, r) = ((g_1, g_2, g_3), (r_1, r_2, r_3)) \in ImL$, we have

$$\begin{aligned} K_P L(u(t)) &= K_P(\dot{u},\ \Delta u) \\ &= \int_0^t \dot{u}(s)ds + \Delta u \\ &= u(t) - u(0) + u(0) - u(\tau) \\ &= u(t) - P(u) \\ &= u(t),\ because\ u \in KerP \end{aligned} \tag{63}$$

and

$$\begin{aligned} LK_P(g(t), r) &= L(\textstyle\int_0^t g(s)ds + r) \\ &= (g(t),\ -\textstyle\int_0^\tau g(t)dt) \\ &= (g(t),\ r)\ because\ (g, r) \in ImL. \end{aligned} \tag{64}$$

Thus,

$$QN \begin{pmatrix} x \\ y \\ z \end{pmatrix} = \left(\begin{pmatrix} A_1 \\ A_2 \\ A_3 \end{pmatrix}, \begin{pmatrix} 0 \\ 0 \\ 0 \end{pmatrix} \right).$$

Furthermore,

$$K_P(I-Q)N\begin{pmatrix}x\\y\\z\end{pmatrix} = K_PN\begin{pmatrix}x\\y\\z\end{pmatrix} - K_PQN\begin{pmatrix}x\\y\\z\end{pmatrix} = \begin{pmatrix}B_1\\B_2\\B_3\end{pmatrix} - \begin{pmatrix}C_1\\C_2\\C_3\end{pmatrix} + \begin{pmatrix}D_1\\D_2\\D_3\end{pmatrix}, \tag{65}$$

where

$$\begin{aligned}
A_1 &= \gamma_S - \omega_S - \mu_S - \frac{1}{\tau}\int_0^\tau (\sigma_G e^{z(t)} + \frac{\gamma_S}{K_T}(e^{x(t)} + e^{y(t)}))dt \\
&\quad + \frac{1}{\tau}\int_0^\tau \gamma_{NS} e^{-x(t)} e^{y(t)} \left(1 - \frac{e^{x(t)} + e^{y(t)}}{K_T}\right) dt + \frac{1}{\tau}\ln(1 - \eta_S w(e^{z(\tau)})), \\
A_2 &= -\mu_{NS} + \frac{1}{\tau}\int_0^\tau \omega_S e^{x(t)} e^{-y(t)} dt, \\
A_3 &= \gamma_G - \mu_G - \frac{1}{\tau}\int_0^\tau \frac{\gamma_G}{K_G} e^{z(t)} dt - \frac{1}{\tau}\int_0^\tau \sigma_{NS} e^{y(t)} dt + \frac{1}{\tau}\ln(1 - \eta_G),
\end{aligned} \tag{66}$$

$$\begin{aligned}
B_1 &= \int_0^t \left(-\omega_S - \mu_S - \sigma_G e^{z(s)} + (\gamma_S + \gamma_{NS} e^{y(s)} e^{-x(s)}) \left(1 - \frac{e^{x(s)} + e^{y(s)}}{K_T}\right)\right) ds, \\
B_2 &= \int_0^t \left(-\mu_{NS} + \omega_S e^{x(s)} e^{-y(s)}\right) ds, \\
B_3 &= \int_0^t \left(\gamma_G \left(1 - \frac{e^{z(s)}}{K_G}\right) - \sigma_{NS} e^{y(s)} - \mu_G\right) ds,
\end{aligned} \tag{67}$$

$$\begin{aligned}
C_1 &= \frac{t}{\tau}\left(\int_0^\tau \left(-\omega_S - \mu_S - \sigma_G e^{z(s)} + (\gamma_S + \gamma_{NS} e^{y(s)} e^{-x(s)}) \left(1 - \frac{e^{x(s)} + e^{y(s)}}{K_T}\right)\right) ds \right. \\
&\quad \left. + \ln(1 - \eta_S w(e^{z(\tau)}))\right), \\
C_2 &= \frac{t}{\tau}\int_0^\tau \left(-\mu_{NS} + \omega_S e^{x(s)} e^{-y(s)}\right) ds, \\
C_3 &= \frac{t}{\tau}\left(\int_0^\tau \left(\gamma_G \left(1 - \frac{e^{z(s)}}{K_G}\right) - \sigma_{NS} e^{y(s)} - \mu_G\right) ds + \ln(1 - \eta_G)\right),
\end{aligned}$$

$$\begin{aligned}
D_1 &= \ln(1 - \eta_S w(e^{z(\tau)})), \\
D_2 &= 0, \\
D_3 &= \ln(1 - \eta_G).
\end{aligned} \tag{68}$$

Clearly, QN and $K_P(I-Q)N$ are continuous then for any open bounded set $\Omega \subset X$, $QN(\bar{\Omega})$ is bounded. Furthermore, let $t_1,\ t_2 \in [0,\ \tau]$, $u(t) = (x, y, z)(t)$,

$$f(t,u(t)) = \begin{pmatrix} -\omega_S - \mu_S - \sigma_G e^z + (\gamma_S + \gamma_{NS} e^y e^{-x}) \left(1 - \dfrac{e^x + e^y}{K_T}\right) \\ -\mu_{NS} + \omega_S e^x e^{-y} \\ \gamma_G \left(1 - \dfrac{e^z}{K_G}\right) - \sigma_{NS} e^y - \mu_G \end{pmatrix}$$

and

$$a = \begin{pmatrix} \ln(1 - \eta_S w(e^{z(\tau)})) \\ 0 \\ \ln(1 - \eta_G) \end{pmatrix}.$$

We have

$$\begin{aligned} &|K_P(I-Q)N(u(t_2)) - K_P(I-Q)N(u(t_1))| \\ &= \left| \int_0^{t_2} f(s,u(s))ds - \int_0^{t_1} f(s,u(s))ds - \frac{t_2}{\tau} \left\{ \int_0^{\tau} f(s,u(s))ds + a \right\} \right. \\ &\quad \left. + \frac{t_1}{\tau} \left\{ \int_0^{\tau} f(s,u(s))ds + a \right\} \right| \\ &\quad \left| \int_{t_1}^{t_2} f(s,u(s))ds - \frac{(t_2 - t_1)}{\tau} \left\{ \int_0^{\tau} f(s,u(s))ds + a \right\} \right| \\ &\leq |t_2 - t_1| \max_{t\in[0,\,\tau]} |f(t,u(t))| + \frac{|t_2 - t_1|}{\tau} \left(\tau \max_{t\in[0,\,\tau]} |f(t,u(t))| + a \right) \\ &\leq |t_2 - t_1| \left(2 \max_{t\in[0,\,\tau]} |f(t,u(t))| + \frac{a}{\tau} \right) \end{aligned} \tag{69}$$

and

$$\begin{aligned} |K_P(I-Q)N(u(t))| &\leq |a| + \tau \max_{t\in[0,\,\tau]} |f(t,u(t))| + |a| + \tau \max_{t\in[0,\,\tau]} |f(t,u(t))| \\ &\leq 2 \left(|a| + \tau \max_{t\in[0,\,\tau]} |f(t,u(t))| \right). \end{aligned} \tag{70}$$

Then using relations (69), (70) and the Arzela–Ascoli's theorem (Sonntag 1997, Theorem 3.1, p. 314) we deduce that $K_P(I-Q)N(\bar{\Omega})$ is compact. Thus, N is a $L-$compact mapping on $\bar{\Omega}$. The isomorphism J of ImQ onto $KerL$ may be defined by

$$J : ImQ \to X, \quad \left(\begin{pmatrix} u \\ v \\ w \end{pmatrix}, \begin{pmatrix} 0 \\ 0 \\ 0 \end{pmatrix} \right) \to \begin{pmatrix} u \\ v \\ w \end{pmatrix}.$$

Now we reach the position to search for an appropriate open, bounded subset Ω for the application of the continuation theorem, i.e. we search M_0 such that every τ-periodic solution of system (1, 2) satisfies $|x(t)| + |y(t)| + |z(t)| \leq M_0$ with $0 \leq t \leq \tau$.

Corresponding to the operator equation $Lx = \beta Nx$, $\beta \in (0, 1)$, we have

$$\begin{cases} \dot{x}(t) = \beta\left[-\omega_S - \mu_S - \sigma_G e^z + (\gamma_S + \gamma_{NS} e^y e^{-x})\left(1 - \dfrac{e^x + e^y}{K_T}\right)\right], \quad t \neq t_n. \\ \dot{y}(t) = \beta\left[-\mu_{NS} + \omega_S e^x e^{-y}\right], \quad t_{n+1} = t_n + \tau, \\ \dot{z}(t) = \beta\left[\gamma_G\left(1 - \dfrac{e^z}{K_G}\right) - \sigma_{NS} e^y - \mu_G\right], \\ x(t^+) - x(t) = \beta \ln(1 - \eta_S w(e^z)), \quad t = t_n. \\ y(t^+) - y(t) = 0, \quad n = 0, 1, 2, \ldots, \\ z(t^+) - z(t) = \beta \ln(1 - \eta_G). \end{cases} \tag{71}$$

Suppose that $(x(t), y(t), z(t)) \in X$ is an arbitrary solution of system (71) for a certain $\beta \in (0, 1)$. Integrating on both sides of (71) over the interval $[0,\ \tau]$, we obtain

$$\begin{cases} \displaystyle\int_0^\tau \left[-\frac{\gamma_S}{K_T}(e^x + e^y) + \gamma_{NS} e^y e^{-x}\left(1 - \frac{e^x + e^y}{K_T}\right) - \sigma_G e^z\right] dt = (\omega_S + \mu_S - \gamma_S)\tau \\ \qquad\qquad - \ln(1 - \eta_S w(e^{z(\tau)})), \\ \displaystyle\int_0^\tau \omega_S e^x e^{-y} dt = \mu_{NS}\tau, \\ \displaystyle\int_0^\tau \left[\frac{\gamma_G}{K_G} e^z + \sigma_{NS} e^y\right] dt = (\gamma_G - \mu_G)\tau + \ln(1 - \eta_G). \end{cases} \tag{72}$$

Note that assumptions of Theorem 2 lead

$$(\gamma_G - \mu_G)\tau + \ln(1 - \eta_G) > 0.$$

Since X is a Banach space and $(x(t), y(t), z(t)) \in X$, there exist $\overline{\xi}$, $\underline{\xi}$, $\overline{\eta}$, $\underline{\eta}$, $\overline{\tau}$ and $\underline{\tau}$ such that

$$\begin{aligned} x(\overline{\xi}) &= \max_{0\le t\le\tau} x(t),\ x(\underline{\xi}) = \min_{0\le t\le\tau} x(t), \\ y(\overline{\eta}) &= \max_{0\le t\le\tau} y(t),\ y(\underline{\eta}) = \min_{0\le t\le\tau} y(t), \\ z(\overline{\tau}) &= \max_{0\le t\le\tau} z(t),\ z(\underline{\tau}) = \min_{0\le t\le\tau} z(t). \end{aligned} \tag{73}$$

It follows from system (72) that

$$\begin{aligned} \int_0^\tau |\dot{x}(t)| dt &\le (\omega_S + \mu_S)\tau + \int_0^\tau \left|-\sigma_G e^z + (\gamma_S + \gamma_{NS} e^y e^{-x})\left(1 - \frac{e^x + e^y}{K_T}\right)\right| dt \\ &\le (\omega_S + \mu_S)\tau + \sigma_G \tau e^{z(\overline{\tau})} + \int_0^\tau (\gamma_S + \gamma_{NS} e^y e^{-x}) dt \\ &\le (\omega_S + \mu_S)\tau + \sigma_G \tau e^{z(\overline{\tau})} + \int_0^\tau (\gamma_S + \gamma_{NS} e^y) dt \\ &\le (\omega_S + \mu_S + \gamma_S)\tau + \sigma_G \tau e^{z(\overline{\tau})} + \gamma_{NS} \tau e^{y(\overline{\eta})}, \end{aligned} \tag{74}$$

$$\begin{aligned} \int_0^\tau |\dot{y}(t)| dt &\le \mu_{NS}\tau + \int_0^\tau |\omega_S e^x e^{-y}| dt \\ &\le 2\mu_{NS}\tau \end{aligned} \tag{75}$$

and

$$\begin{aligned}\int_0^\tau |\dot{z}(t)|dt &\le (\gamma_G+\mu_G)\tau+\int_0^\tau\left(\frac{\gamma_G}{K_G}e^z+\sigma_{NS}e^y\right)dt\\ &\le (\gamma_G+\mu_G)\tau+(\gamma_G-\mu_G)\tau+\ln(1-\eta_G)\\ &\le 2\gamma_G\tau+\ln(1-\eta_G).\end{aligned} \tag{76}$$

Recall that

$$\begin{aligned}\rho_G^0>1 &\Longleftrightarrow (\gamma_G-\mu_G)\tau+\ln(1-\eta_G)>0\\ &\Longrightarrow 2\gamma_G\tau+\ln(1-\eta_G)>0.\end{aligned}$$

Since

$$\begin{aligned}\tau\left(\frac{\gamma_G}{K_G}e^{z(\underline{\tau})}+\sigma_{NS}e^{y(\underline{\eta})}\right) &\le (\gamma_G-\mu_G)\tau-\int_0^\tau\dot{z}(t)dt\\ &\le (\gamma_G-\mu_G)\tau+\ln(1-\eta_G),\end{aligned} \tag{77}$$

then

$$\begin{aligned}z(\underline{\tau}) &\le \ln\left\{\frac{K_G}{\gamma_G}\left((\gamma_G-\mu_G)+\frac{\ln(1-\eta_G)}{\tau}\right)\right\}\\ y(\underline{\eta}) &\le \ln\left\{\frac{1}{\sigma_{NS}}\left((\gamma_G-\mu_G)+\frac{\ln(1-\eta_G)}{\tau}\right)\right\}.\end{aligned} \tag{78}$$

Moreover, from

$$\int_0^\tau \omega_S e^x e^{-y}dt=\mu_{NS}\tau$$

we deduce

$$x(\underline{\xi})\le\ln\left(\frac{\mu_{NS}}{\omega_S}e^{y(\overline{\eta})}\right)\quad\text{and}\quad x(\overline{\xi})\ge\ln\left(\frac{\mu_{NS}}{\omega_S}\right).$$

Furthermore,

$$\int_0^\tau\dot{z}(t)dt=\int_0^\tau\left[\gamma_G-\mu_G-\frac{\gamma_G}{K_G}e^{z(t)}-\sigma_{NS}e^{y(t)}\right]=-\ln(1-\eta_G).$$

Using

$$\begin{aligned}0<(\gamma_G-\mu_G)\tau+\ln(1-\eta_G) &= \int_0^\tau\left[\frac{\gamma_G}{K_G}e^{z(t)}+\sigma_{NS}e^{y(t)}\right]dt\\ &\le \int_0^\tau\left[\frac{\gamma_G}{K_G}e^{z(\overline{\tau})}+\sigma_{NS}e^{y(\overline{\eta})}\right]dt\\ &= \tau\left[\frac{\gamma_G}{K_G}e^{z(\overline{\tau})}+\sigma_{NS}e^{y(\overline{\eta})}\right],\end{aligned} \tag{79}$$

then there exist $\zeta_1>0,\ \zeta_2>0$ such that

- $\zeta_1 + \zeta_2 = (\gamma_G - \mu_G) + \dfrac{\ln(1-\eta_G)}{\tau}$,
- $\dfrac{\gamma_G}{K_G} e^{z(\overline{\tau})} \geq \zeta_1$ and
- $\sigma_{NS} e^{y(\overline{\eta})} \geq \zeta_2$.

Thus,

$$z(\overline{\tau}) \geq \ln\left\{\frac{K_G}{\gamma_G}\zeta_1\right\}, \quad y(\overline{\eta}) \geq \ln\left\{\frac{1}{\sigma_{NS}}\zeta_2\right\}. \tag{80}$$

So, keeping in mind that by assumptions of Theorem 2, one has

$$(\gamma_G - \mu_G) + \frac{\ln(1-\eta_G)}{\tau} > 0, \tag{81}$$

$$\begin{aligned}
x(t) &\leq x(\underline{\xi}) + \int_0^\tau |\dot{x}(t)|dt \\
&\leq \ln\left(\frac{\mu_{NS}}{\omega_S} e^{y(\overline{\eta})}\right) + (\omega_S + \mu_S + \gamma_S)\tau + \sigma_G \tau e^{z(\overline{\tau})} + \gamma_{NS}\tau e^{y(\overline{\eta})} := x_u, \\
y(t) &\leq y(\underline{\eta}) + \int_0^\tau |\dot{y}(t)|dt \\
&\leq \ln\left\{\frac{1}{\sigma_{NS}}\left((\gamma_G - \mu_G) + \frac{\ln(1-\eta_G)}{\tau}\right)\right\} + 2\mu_{NS}\tau := y_u, \\
z(t) &\leq z(\underline{\tau}) + \int_0^\tau |\dot{z}(t)|dt \\
&\leq \ln\left\{\frac{K_G}{\gamma_G}\left((\gamma_G - \mu_G) + \frac{\ln(1-\eta_G)}{\tau}\right)\right\} + 2\gamma_G\tau + \ln(1-\eta_G) := z_u, \\
x(t) &\geq x(\overline{\xi}) - \int_0^\tau |\dot{x}(t)|dt \\
&\geq \ln\left(\frac{\mu_{NS}}{\omega_S}\right) - (\omega_S + \mu_S + \gamma_S)\tau - \sigma_G \tau e^{z(\overline{\tau})} - \gamma_{NS}\tau e^{y(\overline{\eta})} := x_l, \\
y(t) &\geq y(\overline{\eta}) - \int_0^\tau |\dot{y}(t)|dt \\
&\geq \ln\left\{\frac{\zeta_2}{\sigma_{NS}}\right\} - 2\mu_{NS}\tau := y_l, \\
z(t) &\geq z(\overline{\tau}) - \int_0^\tau |\dot{z}(t)|dt \\
&\geq \ln\left\{\frac{K_G}{\gamma_G}\zeta_1\right\} - 2\gamma_G\tau - \ln(1-\eta_G) := z_l,
\end{aligned} \tag{82}$$

therefore we obtain,

$$\begin{aligned}
&\max_{0\le t\le\tau}|x(t)| \le \max\{|x_u|,|x_l|\} := M_x,\\
&\max_{0\le t\le\tau}|y(t)| \le \max\{|y_u|,|y_l|\} := M_y,\\
&\max_{0\le t\le\tau}|z(t)| \le \max\{|z_u|,|z_l|\} := M_z.
\end{aligned} \tag{83}$$

M_x, M_y and M_z are independent of β. Now let us consider the algebraic equations

$$\begin{cases}
\gamma_S-\omega_S-\mu_S+\dfrac{1}{\tau}\ln(1-\eta_S w(e^{z(\tau)}))\\
-\dfrac{1}{\tau}\displaystyle\int_0^\tau\left[\frac{\gamma_S}{K_T}(e^x+e^y)-\beta\gamma_{NS}e^y e^{-x}\left(1-\frac{e^x+e^y}{K_T}\right)+\beta\sigma_G e^z\right]dt = 0,\\
-\mu_{NS}+\dfrac{1}{\tau}\displaystyle\int_0^\tau\omega_S e^x e^{-y}dt = 0,\\
(\gamma_G-\mu_G)+\dfrac{1}{\tau}\ln(1-\eta_G)-\dfrac{1}{\tau}\displaystyle\int_0^\tau\left[\frac{\gamma_G}{K_G}e^z+\sigma_{NS}e^y\right]dt = 0
\end{cases} \tag{84}$$

for $(x, y, z) \in \mathbb{R}^3$, where $\beta \in [0,\ 1]$ is a parameter. By carrying out similar arguments as in system (72), one can show that any solution (x^*, y^*, z^*) of (84) with $\beta \in [0,\ 1]$ satisfies

$$l_1 \le x^* \le L_1, \quad l_2 \le y^* \le L_2, \quad l_3 \le z^* \le L_3. \tag{85}$$

Taking $M_0 = M_x + M_y + M_z + M_k$ where $M_k > 0$ is taken sufficiently large such that $M_k > |l_1| + |L_1| + |l_2| + |L_2| + |l_3| + |L_3|$, we define $\Omega = \left\{(x, y, z)^T \in X : ||(x, y, z)|| < M_0\right\}$, then Ω verifies the requirement (1) of the continuation theorem (Gaines and Mawhin 1977, page 40). When $(x, y, z) \in \partial\Omega \cap KerL = \partial\Omega \cap \mathbb{R}^3$, (x, y, z) is a constant vector in $\mathbb{R}^3$ with $||(x, y, z)|| = M_0$. Then from (85) and the definition of M_0, one has

$$QN\begin{pmatrix}x\\y\\z\end{pmatrix} = \left(\begin{pmatrix}A^{(1)}\\A^{(2)}\\A^{(3)}\end{pmatrix}, \begin{pmatrix}0\\0\\0\end{pmatrix}\right) \neq \left(\begin{pmatrix}0\\0\\0\end{pmatrix}, \begin{pmatrix}0\\0\\0\end{pmatrix}\right), \tag{86}$$

where,

$$\begin{aligned}
A^{(1)} &= \gamma_S-\omega_S-\mu_S-\frac{1}{\tau}\int_0^\tau\left(\sigma_G e^z+\frac{\gamma_S}{K_T}(e^x+e^y)\right)dt\\
&\quad+\frac{1}{\tau}\int_0^\tau\gamma_{NS}e^{-x}e^y\left(1-\frac{e^x+e^y}{K_T}\right)dt\\
&\quad+\frac{1}{\tau}\ln(1-\eta_S w(e^{z(\tau)})),\\
A^{(2)} &= -\mu_{NS}+\frac{1}{\tau}\int_0^\tau\omega_S e^x e^{-y}dt,\\
A^{(3)} &= \gamma_G-\mu_G-\frac{1}{\tau}\int_0^\tau\frac{\gamma_G}{K_G}e^z dt-\frac{1}{\tau}\int_0^\tau\sigma_{NS}e^y dt+\frac{1}{\tau}\ln(1-\eta_G),
\end{aligned} \tag{87}$$

that is, the first part of (2) of the continuation theorem (Gaines and Mawhin 1977, page 40) is valid.

To compute the Brouwer degree, let us consider the homotopy

$$H_\beta((x, y, z)^T) = \beta JQN((x, y, z)^T) + (1-\beta)V((x, y, z)^T), \quad \beta \in [0,\ 1],$$

where

$$V((x, y, z)^T) = \begin{pmatrix} \gamma_S - \omega_S - \mu_S + \dfrac{1}{\tau}\ln\left(1 - \eta_S w(e^{z(\tau)})\right) - \dfrac{\gamma_S}{K_T}(e^x + e^y) \\ -\mu_{NS} + \omega_S e^x e^{-y} \\ (\gamma_G - \mu_G) + \dfrac{1}{\tau}\ln(1-\eta_G) - \dfrac{\gamma_G}{K_G}e^z - \sigma_{NS}e^y \end{pmatrix}.$$

From (84), it follows that $0 \notin H_\beta(\partial\Omega \cap KerL)$ for $\beta \in [0,\ 1]$. Moreover, since $-\dfrac{\gamma_S\gamma_G(\omega_S + \mu_{NS})}{K_T K_G} \neq 0$, the algebraic equation $V((x, y, z)^T) = 0$ has a unique solution $(e^{x^*}, e^{y^*}, e^{z^*})^T \in \mathbb{R}^3$. We compute the Brouwer degree $(deg(\cdot,\cdot,\cdot))$ by using the invariance property of homotopy (Fan and Kuang 2004), one has

$$\begin{aligned} deg(JQN, \Omega \cap KerL, 0) &= deg(V, \Omega \cap KerL, 0) \\ &= \sum_{p \in V^{-1}(0)} sign(J_V(p)) \\ &= sign\left[\det\begin{pmatrix} -\dfrac{\gamma_S}{K_T}e^{x^*} & -\dfrac{\gamma_S}{K_T}e^{y^*} & 0 \\ \mu_{NS} & -\mu_{NS} & 0 \\ 0 & -\sigma_{NS}e^{y^*} & -\dfrac{\gamma_G}{K_G}e^{z^*} \end{pmatrix}\right] \\ &= sign\left[-\frac{\gamma_G\gamma_S}{K_T K_G}(\mu_{NS} + \omega_S)e^{x^*}e^{z^*}\right], \text{ since } \omega_S e^{x^*} \\ &= \mu_{NS}e^{y^*} \\ &= -1 \neq 0. \end{aligned} \tag{88}$$

By now, we have proved that Ω verifies all requirements of the continuation theorem (Gaines and Mawhin 1977, page 40), then $Lx = Nx$ has at least one solution in $DomL \cap \overline{\Omega}$, i.e. system (62) has at least one solution in $DomL \cap \overline{\Omega}$, say $(x^*(t), y^*(t), z^*(t))$. Set $T_S^*(t) = \exp(x^*(t))$, $T_{NS}^*(t) = \exp(y^*(t)$, $G^*(t) = \exp(z^*(t))$, then $(T_S^*(t), T_{NS}^*(t), G^*(t))$ is a positive and τ-periodic solution of system (1, 2). This completes the proof.

11 Particular values of σ_{NS}, σ_G and τ

With respect to relations (13) and (17), we set

$$\begin{cases} \sigma_G^\star(\tau) = \dfrac{1}{G_{int}}\left(\gamma_S - (\mu_S + \omega_S + \mu_{NS})\right), \\ \qquad\quad = \dfrac{(\gamma_S - (\mu_S + \omega_S + \mu_{NS}))}{\dfrac{K_G}{\gamma_G}\left(\gamma_G - \mu_G + \dfrac{\ln(1-\eta_G)}{\tau}\right)}, \\ \sigma_{NS}^\star(\tau) = \dfrac{1}{\overline{T}_{NS}}\left(\gamma_G - \mu_G + \dfrac{\ln(1-\eta_G)}{\tau}\right), \\ \tau^\star = -\dfrac{\ln(1-\eta_G)}{\gamma_G\left(1 - \dfrac{1}{\mathcal{R}_T^G}\right)}. \end{cases} \tag{89}$$

One can note that $\sigma_G^\star$, $\sigma_{NS}^\star$ and $\tau^\star$ determined regions of stability/instability of forest and grassland solutions, with respect to σ_G, σ_{NS} and τ variations.

References

Abbadie L, Gignoux J, Le Roux X, Lepage M (2006) Lamto: structure, functioning, and dynamics of a Savanna Ecosystem. Eco, Stu, Springer, New York

Accatino F, De Michele C (2013) Humid savanna-forest dynamics: a matrix model with vegetation-fire interactions and seasonality. Ecol Model 265:170–179

Accatino F, De Michele C, Vezzoli R, Donzelli D, Scholes R (2010) tree-grass co-existence in savanna: interactions of rain and fire. J Theor Biol 267:235–242

Accatino F, Wiegand K, Ward D, De Michele C (2016) Trees, grass, and fire in humid savannas: the importance of life history traits and spatial processes. Ecol Model 320:135–144

Anguelov R, Dumont Y, Lubuma JM-S (2012) On nonstandard finite difference schemes in biosciences. AIP Conf Proc 1487:212–223

Anguelov R, Dumont Y, Lubuma JM-S, Mureithi E (2013) Stability analysis and dynamics preserving non-standar finite difference schemes for malaria model. Math Popul Stud 20(2):101–122

Anguelov R, Dumont Y, Lubuma JM-S, Shillor M (2014) Dynamically consistent nonstandard finite difference schemes for epidemiological Models. J Comput Appl Math 255:161–182

Archibald S, Roy DP, Van Wilgen B, Scholes RJ (2009) What limits fire? An examination of drivers of burnt area in Southern Africa. Global Change Biol 15:613–630

Augier P, Lett C, Poggiale JC (2010) Modélisation mathématique en écologie. Cours et exercices corrigés. Dunod, Paris

Bainov DD, Simeonov PS (1995) Impulsive differential equations: asymptotic properties of the solutions. World scientific publishing Co, Singapore

Barbier N, Couteron P, Lefever R, Deblauwe V, Lejeune O (2008) Spatial decoupling of facilitation and competition at the origin of gapped vegetation patterns. Ecology 89:1521–1531

Baudena M, D'Andrea F, Provenzale A (2010) An idealized model for tree-grass coexistence in savannas: the role of life stage structure and fire disturbances. J Ecol 98:74–80

Baudena M, Rietkerk M (2013) Complexity and coexistence in a simple spatial model for arid savanna ecosystems. Theor Ecol 6:131–141

Baudena M, Dekker SC, van Bodegom PM, Cuesta B, Higgins SI, Lehsten V, Reick CH, Rietkerk M, Scheiter S, Yin Z, Zavala MA, Brovkin V (2014) Forest, Savannas and grasslands: bridging the knowledge gap between ecology and dynamic global vegetation models. Biogeosci Discuss 11:9471–9510

Beckage B, Gross LJ, Platt WJ (2011) Grass feedbacks on fire stabilize savannas. Ecol Model 222:2227–2233

Belsky AJ (1994) Influuences of trees on savanna productivity: tests of shade, nutrients and tree-grass competition. Ecology 75:922–932

Belsky AJ, Amundson RG, Duxbury JM, Rika SJ, Ali AR, Mwonga SM (1989) The effects of trees on their physical, chemical, and biological environment in a semi-arid savanna in Kenya. J Appl Ecol 26:1005–1024
Bond WJ (2008) What limits trees in C4 grasslands and savannas ? Annu Rev Ecol Evol Syst 39:641–59
Bond WJ, Keeley JE (2005) Fire as a global herbivore: the ecology and evolution of flammable ecosystems. Trends Ecol Evol 20:387–394
Bond WJ, Midgley GF, Woodward FI (2003) What controls South African vegetation-climate or fire? S Afr J Bot 69:79–91
Bond WJ, Woodward FI, Midgley GF (2005) The global distribution of ecosystems in a world without fire. New Phytol 165:525–538
Breman H and Kessler JJ (1995) Woody plants in agroecosystems of semi-arid regions. With an emphasis on the Sahelian countries. Advanced series in Agricultural, vol 23, Springer, Berlin
Calabrese JM, Vazquez F, López C, San M, Miguel Grimm V (2010) The independent and interactive effects of tree-tree establishment competition and fire on Savanna structure and dynamics. Am Nat 175:E44–E65
Chen Y, Liu Z, Haque M (2009) Analysis of a Leslie-Gower-type prey-predator model with periodic impulsive perturbations. Commun Nonlinear Sci Numer Simul 14:3412–3423
Couteron P, Kokou K (1997) Woody vegetation spatial patterns in a semi-arid savanna of Burkina Faso, West Africa. Plant Ecol 132:211–227
Dai C, Zhao M, Chen L (2012) Dynamic complexity of an Ivlev-type prey-predator system with impulsive state feedback control. J Appl Math 17:1–17 (Article ID 534276)
Deblauwe V, Barbier N, Couteron P, Lejeune O, Bogaert J (2008) The global biogeography of semi-arid periodic vegetation patterns. Global Ecol Biogeogr. doi:10.1111/j.1466-8238.2008.00413.x
De Michele C, Accatino F, Vezzoli R, Scholes RJ (2011) Savanna domain in the herbivores-fire parameter space exploiting a tree-grass-soil water dynamic model. J Theor Biol 289:74–82
Diouf A, Barbier N, Lykke AM, Couteron P, Deblauwe V, Mahamane A, Saadou M, Bogaert J (2012) Relationships between fire history, edaphic factor and woody vegetation structure and composition in a semi-arid savanna landscape (Niger, West Africa). Appl Veg Sci 15:488–500
D'Odorico P, Laio F, Ridolfi LA (2006) probabilistic analysis of fire-induced tree-grass coexistence in savannas. Am Nat 167:E79–E87
D'Onofrio D (2002) Stability properties of pulse vaccination strategy in SEIR epidemic model. Math Biosci 179:57–72
Dumont Y, Russell JC, Lecomte V, Le Corre M (2010) Conservation of endangered endemic seabirds within a multi-predator context: the Barau's petrel in Réunion island. Nat Ressour Model 23:381–436
Dumont Y, Tchuenche JM (2012) Mathematical studies on the sterile insect technique for the chikungunya disease and aedes albopictus. J Math Biol 65(5):809–854
Fan M, Kuang Y (2004) Dynamics of a nonautonomous predator-prey system with the Beddington-DeAngelis functional response. J Math Anal Appl 295:15–39
Favier C, Aleman J, Bremond L, Dubois MA, Freycon V, Yangakola JM (2012) Abrupt shifts in African Savanna tree cover along a climatic gradient. Glob Ecol Biogeogr 21:787–797
February EC, Higgins SI, Bond WJ, Swemmer L (2013) Influence of competition and rainfall manipulation on the growth responses of savanna trees and grasses. Ecology 94(5):1155–1164
Fernandez-Oto C, Tlidi M, Escaff D, Clerc MG (2014) Strong interaction between plants induces circular barren patches: fairy circles. Phil Trans R Soc A 372(2027):20140009
Frost PGH, Robertson F (1985) The ecological effects of fire in savannas. In: Walker BH (ed) Determinants of tropical savannas, vol 3., Monograph seriesInternational Council of Scientific Unions Press, Miami, pp 93–140
Gaines RE, Mawhin J (1977) Coincidence degree and nonlinear differential equations. Springer, New York
Gignoux J (1994) Modélisation de la coexistence herbes-arbres en savane, PhD Thesis
Gignoux J, Lahoreau G, Julliard R, Barot S (2009) Establishment and early persistence of tree seedlings in an annually burned savanna. J Ecol 97:484–495
Gilad E, Shachak M, Meron E (2007) Dynamics and spatial organization of plant communities in water-limited systems. Theor Popul Biol 72:214–230
Govender N, Trollope WSW, Van Wilgen BW (2006) The effect of fire season, fire frequency, rainfall and management on fire intensity in savanna vegetation in South Africa. J Appl Ecol 43:748–758
Hale JK (1980) Ordinary differential equations, 2nd edn. Krieger Publishing Company, Malabar
Hale JK (1988) Asymptotic behavior of dissipative systems. American Mathematical Society, Providence

Higgins SI, Bond WJ, Trollope WSW (2000) Fire, resprouting and variability: a recipe for grass-tree coexistence in savanna. J Ecol 88:213–229
Higgins SI, Bond WJ, Trollope WSW, Williams RJ (2008) Physically motivated empirical models for the spread and intensity of grass fires. Int J Wildland Fire 17:595–601
Higgins SI, Shackleton CM, Robinson ER (1999) Changes in woody community structure and composition under constrasting landuse systems in a semi-arid Savanna, South Africa. J Biogeo 26:619–627
Hirota M, Holmgren M, Van Nes EH, Scheffer M (2011) Global resilience of tropical forest and Savanna to critical transitions. Science 334:232
Hoffmann WA, Solbrig OT (2003) The role of topkill in the differential response of savanna woody species to fire. For Ecol Manag 180:273–286
Jeffery KJ, Korte L, Palla F, Walters G, White LJT, Abernethy KA (2014) Fire management in a changing landscape: a case study from Lopé national park. Gabon Parks 20(1):39–52
Lefever R, Barbier N, Couteron P, Lejeune O (2009) Deeply gapped vegetation patterns: oncrown/root allometry, criticality and desertification. J Theo Ecol 261:194–209
Lehmann C, Prior LD, Williams RJ, Bowman DMJS (2008) Spatio-temporal trends in tree cover of a tropical mesic savanna are driven by landscape disturbance. J Appl Ecol 45:1304–1311
Maurin O, Davies TJ, Burrows JE, Daru BH, Yessoufou K, Muasya AM, Van der Bank M, Bond JW (2014) Savanna fire and the origins of the underground forests of Africa. New Phytologist 204(1):201–214
Menaut JC (1983) The vegetation of african savannas. In: Bourlière F (ed) Tropical Savannas, vol 13., Ecosystems of the worldElsevier, Amsterdam, pp 109–149
Menaut JC, César J (1979) Structure and primary productivity of Lamto savannas, Ivory Coast. Ecology 60:1197–1210
Mermoz S, Réjou-Méchan M, Villard L, Le Toant T, Rossi V, Gourlet-Fleury S (2015) Decrease of L-band SAR backscatter with biomass of dense forests. Rem Sens Environ 159:307–317
Mermoz S, Le Toant T, Villard L, Réjou-Méchan M, Seifert-Granzin J (2014) Biomass assessment in the Cameroon savanna using ALOS PALSAR data. Rem Sens Environ. doi:10.1016/j.rse.2014.01.029
Mordelet P, Menaut JC (1995) Influence of trees on above-ground production dynamics of grasses in a humid savanna. J Veg Sci 6:223–228
Moro MJ, Pugnaire FI, Haase P, Puigdefabregas J (1997) Effect of the canopy of Retama spaerocarpa on its understorey in a semi-arid environment. Funct Ecol 11:425–431
Moustakas A, Kunin WE, Cameron TC, Sankaran M (2013) Facilitation or Competition? Tree Effects on Grass Biomass across a Precipitation Gradient. PLoS One 8(2):e57025
Penning de Vries FWT and Djiteye MA (1982) La productivité des paturages sahéliens. Une étude des sols, des végétations et de l'exploitation de cette ressource naturelle. PUDOC, Wageningen
Pueyo Y, Kefi S, Alados C, Rietkerk M (2008) Dispersal strategies and spatial organization of vegetation in arid ecosystems. Oikos 117:1522–1532
Pueyo Y, Kefi S, Daz-Sierra R, Alados C, Rietkerk M (2010) The role of reproductive plant traits and biotic interactions in the dynamics of semi-arid plant communities. Theor Popul Biol 78:289–297
Sankaran M, Hanan NP, Scholes RJ, Ratnam J, Augustine DJ, Cade BS, Gignoux J, Higgins SI, LeRoux X, Ludwig F, Ardo J, Banyikwa F, Bronn A, Bucini G, Caylor KK, Coughenour MB, Diouf A, Ekaya W, Feral CJ, February EC, Frost PGH, Hiernaux P, Hrabar H, Metzger KL, Prins HHT, Ringrose S, Sea W, Tews J, Worden J, Zambatis N (2005) Determinants of woody covering African savannas. Nature 438:846–849
Sankaran M, Ratnam J, Hanan N (2008) Woody cover in African Savannas: the role of resources, fire and herbivory. Glob Ecol Biogeogr 17:236–245
Scheiter S, Higgins SI (2007) Partitioning of root and shoot competition and the stability of Savannas. Am Nat 170:587–601
Scholes RJ (2003) Convex relationships in ecosystems containing mixtures of trees and grass. Environ Ressour Econ 26:559–574
Scholes RJ, Archer SR (1997) tree-grass interactions in savannas. Annu Rev Ecol Syst 28:517–544
Scholes RJ, Walker BH (1993) An African savanna: synthesis of the Nylsvley study. Cambridge Studies in Applied Ecology and Resource Management. Cambridge University Press, Cambridge, UK
Smit IPJ, Asner G, Govender N, Kennedy-Bowdoin T, Knapp D, Jacobson J (2010) Effects of fire on woody vegetation structure in African savanna. Ecol Appl 20(7):1865–1875
Smit GN, Rethman NFG (2000) The influence of tree thinning on the soil water in a semi-arid savanna of southern Africa. J Arid Environ 44:41–59

Sonntag Y (1997) Topologie et analyse fonctionnelle. Cours de Licence avec 240 exercices et 30 problèmes corrigés. Ellipses Collection Université, p 512
Staver AC, Archibald S, Levin S (2011) Tree cover in sub-Saharan Africa: rainfall and fire constrain forest and Savanna as alternative stable states. Ecology 92(5):1063–1072
Staver AC, Bond WJ (2014) Is there a browse trap ? Dynamics of herbivore impacts on trees and grasses in an African savannas. J Ecol 102:595–602
Staver AC, Levin S (2012) Integrating theoretical climate and fire effects on savanna and forest systems. Am Nat 180(2):211–224
Synodinos AD, Tietjen B, Jeltsch F (2015) Facilitation in drylands: modeling a neglected driver of Savanna dynamics. Ecol Model 304:11–21
Tchuinté A, Tewa JJ, Couteron P, Bowong S, Dumont Y (2014) A generic modeling of fire impact in a tree-grass Savanna model. Biomath 3:1407191
Tilman D (1994) Competition and biodiversity in spatially structured habitats. Ecology 75:2–16
Trollope WSW (1984) Fire in savannas. In: de Booysen PV, Tainton NM (eds) Ecological effects of fire in South African ecosystems. Ecological Studies series, vol 48. Spinger-Verlag, Berlin, pp 149–176
Trollope WSW (1996) Behaviour, effects and use of fire in the savannas of southern Africa. In: Grice TC, Slatter SM (eds) Fire in the management of northern Australian pastoral lands. Proceedings of the Tropical Grassland Society of Australia, vol 8, pp 9–23
Trollope WSW, and Trollope LA (1996) Fire in African savanna and other grazing ecosystems. Paper presented at the seminar on 'Forest fire and global change' held in Shshenkoye in the Russian Federation, 4–10 August
Tschinkel WR (2012) The life cycle and life span of Namibian fairy circles. PLoS One 7(6):e38056
Van de Vijver CA, Foley Olff H (1999) Changes in the woody component of an East African savanna during 25 years. J Trop Ecol 15:545–564
Van Langevelde F, Van de Vijver C, Kumar L, Van de Koppel J, de Ridder N, Van Andel J et al (2003) Effects of fire and herbivory on the stability of savanna ecosystems. Ecology 84(2):337–350
Van Wilgen BW, Govender N, Biggs HC, Ntsala D, Funda XN (2004) Response of savanna fire regimes to changing fire-management policies in a large African national park. Conserv Biol 18(6):1537–1540
Wakeling JL, Staver AC, Bond WJ (2011) Simply the best: the transition of savanna saplings to trees. Oikos 120:1448–1451
Walker B, Ludwig D, Holling CS, Peterman RM (1981) Stability of semi-arid savanna grazing systems. J Ecol 69:473–498
Weltzin JF, Coughenour MB (1990) Savanna tree influence on understory vegetation and soil nutrients in northwestern Kenya. J Veg Sci 1:325–334
Yatat V, Dumont Y, Tewa JJ, Couteron P, Bowong S (2014) Mathematical analysis of a size structured tree-grass competition model for Savanna ecosystems. Biomath 3:1404212